Supporting Information

Phosphorescence Properties of Boron β-Diketiminate Complexes Modulated by Spiro Structures

Keisuke Suwa,[1] Shunichiro Ito,[1,2] Kazuo Tanaka*[1,2]

[1] *Department of Polymer Chemistry, Graduate School of Engineering, Kyoto University, Nishikyo-ku, Katsura, Kyoto 615-8510, Japan.*

[2] *Department of Technology and Ecology, Graduate School of Global Environmental Studies, Kyoto University, Katsura, Nishikyo-ku, Kyoto 615-8510, Japan*

E-mail: tanaka@poly.synchem.kyoto-u.ac.jp

Table of Contents

1. Experimental Section *3*

General experimental details **3**

Materials **5**

2. Synthetic Procedures and Characterization *6*

Synthesis of 4-methyl-*N*-mesitylbenzenamine (Mes_imine) **6**

Synthesis of *N*-mesitylbenzimidoyl chloride (Mes_Cl) **6**

Synthesis of Mes_L **7**

Synthesis of Mes_cat **8**

Synthesis of Mes_naph **9**

Synthesis of Mes_FL **10**

Synthesis of Ph_FL **12**

Synthesis of Ph_FLBr **13**

3. Photophysical Properties *16*

Kinetics of Photophysical Processes **17**

4. Single Crystal X-ray Analysis *18*

5. Powder X-Ray Diffraction *22*

6. DFT Calculations *23*

7. NMR Charts *47*

8. References *57*

1. Experimental Section

General experimental details

^{1}H (400 or 600 MHz) and $^{13}C\{^{1}H\}$ (100 or 150 MHz) NMR spectra were recorded on JEOL JNM-ECZ400, JNM-ECZ400S, and JNM-ECX400P spectrometers. In ^{1}H and $^{13}C\{^{1}H\}$ NMR spectra, tetramethylsilane (TMS) and/or residual solvent peaks were used as an internal standard. In $^{11}B\{^{1}H\}$ NMR spectra, $BF_3 \cdot OEt_2$ in a capillary was used as an external standard. High-resolution mass spectrometry (HRMS) was performed at the Technical Support Office (Department of Synthetic Chemistry and Biological Chemistry, Graduate School of Engineering, Kyoto University), and the HRMS spectra were obtained on a Thermo Fisher Scientific EXACTIVE spectrometer for electrospray ionization (ESI) and for direct analysis in real time (DART). UV–vis absorption spectra were recorded on a SHIMADZU UV-3600i Plus spectrophotometer. Fluorescence and phosphorescence (PL) emission spectra and phosphorescence decay were measured with a HORIBA JOBIN YVON Fluorolog-3 spectrofluorometer and Oxford Optistat DN for temperature control. Absolute PL quantum yields were measured with Hamamatsu Photonics Quantaurus-QY Plus C13534-01. PL lifetimes were measured by a HORIBA FluoroCube spectrofluorometer system and excitation was carried out at 369 nm using a

UV diode laser (NanoLED 369 nm) or a HORIBA DeltaFlex spectrofluorometer system and excitation was carried out at 375 nm using a UV diode laser (DeltaDiode 375 nm)

Materials

All reactions were performed under nitrogen atmosphere using modified Schlenk line techniques. Compounds **Ph_L**[1,2] and *N*-(2,4,6-trimethylphenyl)benzamide[3] were synthesized according to the literatures. Column chromatography was performed with Wakogel C-200 SiO_2. Acetophenone (Tokyo Chemical Industry Co, Ltd.; TCI), aniline (FUJIFILM Wako Pure Chemical Corporation; Wako), benzoyl chloride (TCI), 2,4,6-trimethylaniline (TCI), *p*-toluenesulfonic acid monohydrate (TCI), thionyl chloride (TCI), 1.0 mol/L boron tribromide, dichloromethane solution (Wako), 1.0 mol/L boron trichloride, heptane solution (Sigma-Aldrich), catechol (TCI), 2,3-dihydroxynaphthalene (TCI), 9,9-dimethyl-9*H*-9-ssilafluorene (TCI), 4,4'-dibromo-2,2'-diiodobiphenyl (BLD pharm), triphenylborane–pyridine complex (TCI), lithium diisopropylamide, in *n*-hexane-tetrahydrofuran, 1.0 mol/L (Kanto Chemical Co., Inc.; Kanto), *n*-butyllithium, in *n*-hexane, 1.6 mol/L (Kanto), deoxygenated toluene (Wako), deoxygenated dichloromethane (Wako) and deoxygenated hexane (Wako) were purchased from the commercial sources and used as received. Diethyl ether (Wako), THF (Wako) and triethylamine (Wako) was purified using two-column solid-state purification system (Glasscontour System, Joerg Meyer, Irvine, CA).

2. Synthetic Procedures and Characterization

Synthesis of 4-methyl-*N*-mesitylbenzenamine (Mes_imine)

A 300 mL two-neck round bottom flask equipped with a stirring bar, a Dean–Stark apparatus and a reflux condenser was charged with *p*-toluenesulfonic acid monohydrate (2.10 g, 11.0 mmol) at room temperature. After the flask was sealed with a septum and was evacuated and refilled with nitrogen, to the flask was added acetophenone (13.0 mL, 13.4 g, 111.4 mmol), 2,4,6-trimethylaniline (15.5 mL, 14.9 g, 110 mmol) deoxygenated toluene (150 mL) at room temperature. The reaction mixture was stirred at reflux temperature for 1 day, and the flask was cooled to room temperature. Saturated $NaHCO_3$ aq. was added to the resulting mixture in a separation funnel. The combined organic layer was washed with brine, then dried over anhydrous $MgSO_4$. The mixture was filtered, and all volatiles were removed with a rotary evaporator. The obtained oil was purified by bulb-to-bulb distillation using a Buch GKR-50 glass tube oven at 180 °C to give desired product as a brown oil (19.2 g, 73%). ^{1}H NMR ($CDCl_3$): δ 8.04–8.02 (m, 2H), 7.50–7.45 (m, 3H), 6.89 (s, 2H), 2.30 (s, 3H), 2.07 (s, 3H), 2.00 (s, 6H). $^{13}C\{^1H\}$ NMR ($CDCl_3$): δ 165.6, 146.6, 139.4, 132.0, 130.5, 128.6, 128.5, 127.2, 125.7, 20.9, 18.0, 17.5. HRMS (ESI) $[M+H]^+$: Found, 238.1589; Calcd., 238.1590.

Synthesis of *N*-mesitylbenzimidoyl chloride (Mes_Cl)

A 50 mL two-neck round bottom flask equipped with a stirring bar was charged with *N*-mesitylbenzamide (4.51 g, 18.8 mmol) at room temperature. After the flask was sealed with a septum and was evacuated and refilled with nitrogen, to the flask was added deoxygenated toluene (10.0 mL), and then thionyl chloride (10.0 mL, 16.4 g, 137.9 mmol) at room temperature. The reaction mixture was stirred at 90 °C for 3 h. After the solution was cooled to 70 °C, the solvent and the remaining thionyl chloride were removed by vacuum distillation. Sodium hydrogen carbonate and dichloromethane were added to the residue for neutralization. Precipitates were removed by filtration, and then the solvent was removed by a rotary evaporator to give desired product as a white solid. The product was used for next reaction without further purification.

Synthesis of Mes_L

A 100 mL two-neck round bottom flask equipped with a stirring bar was charged with 4-methyl-*N*-mesitylbenzenamine (3.13 g, 13.1 mmol) at room temperature. After the flask was sealed with a septum and was evacuated and refilled with nitrogen, to the flask was added deoxygenated Et_2O (15.0 mL) at room temperature, and then lithium diisopropylamide (15.0 mL, 15.0 mmol) at –78 °C over 10 min. The reaction mixture was stirred at room temperature for 3 h, and then *N*-mesitylbenzimidoyl chloride (3.49 g, 13.6 mmol) in deoxygenated Et_2O (20.0 mL) was added to the solution at –78 °C. After stirred

the solution at room temperature for 15 h, the solution was poured into a large amount of chloroform. Saturated $NaHCO_3$ aq. was added to the resulting mixture in a separation funnel. The combined organic layer was washed with brine, then dried over anhydrous Na_2SO_4. The mixture was filtered, and all volatiles were removed with a rotary evaporator. The resulting mixture was diluted with a small amount of chloroform and poured into an excess amount of methanol at room temperature, and the precipitate was dried in vacuum to afford the titled compound as a yellow powder (1.81 g, 30%). ^{1}H NMR ($CDCl_3$): δ 12.72 (s, 1H), 7.30–7.27 (m, 4H), 7.22–7.15 (m, 6H), 5.33 (s, 1H), 2.17 (s, 6H), 2.12 (s, 12H). $^{13}C\{^1H\}$ NMR ($CDCl_3$): δ 162.7, 141.1, 139.0, 133.1, 131.0, 128.5, 128.3, 127.6, 127.6, 96.9, 20.7, 18.8. HRMS (ESI) $[M+H]^+$: Found, 459.2789; Calcd., 459.2795.

Synthesis of Mes_cat

A two-neck test tube equipped with a stirring bar was charged with **Mes_FL** (0.050 g, 0.11 mmol) at room temperature. After the flask was sealed with a septum and was evacuated and refilled with nitrogen, to the flask was added deoxygenated dichloromethane (1.0 mL) and then boron tribromide (0.15 mL, 0.15 mmol) at room temperature. The reaction mixture was stirred at room temperature for 1 day, and then catechol (0.014 g, 0.16 mmol) in deoxygenated toluene (7.0 mL) was added to the

solution at room temperature. After stirred the solution at room temperature for 1 day, the solvent was removed with a vacuum pump. The precipitate was diluted with toluene, then the mixture was filtered, and all volatiles were removed with a rotary evaporator. The obtained residue was diluted with a small amount of dichloromethane and poured into an excess amount of ethanol at –78 °C. The precipitate was dried in vacuum to afford the titled compound as a pale yellow powder (1.6 mg, 3.2%). ^{1}H NMR (CD_2Cl_2): δ 7.30–7.19 (m, 10H), 6.61 (s, 4H), 6.31–6.22 (m, 4H), 5.59 (s, 1H), 2.29 (s, 12H), 2.07 (s, 6H). ^{13}C{^{1}H} NMR (CD_2Cl_2): δ 164.7, 151.3, 137.5, 136.6, 136.1, 135.6, 129.2, 128.4, 127.6, 127.6, 118.0, 107.3, 98.6, 20.5, 19.1. ^{11}B{^{1}H} NMR (128 MHz, CD_2Cl_2,): δ 8.45. HRMS (ESI) $[M+Na]^+$: Found, 599.2847; Calcd., 599.2840.

Synthesis of Mes_naph

A 100 mL Schlenk flask equipped with a stirring bar was charged with **Mes_FL** (0.49 g, 1.06 mmol) at room temperature. After the flask was evacuated and refilled with nitrogen, to the flask was added deoxygenated dichloromethane (10.0 mL) and then boron tribromide (1.5 mL, 1.5 mmol) at room temperature. The reaction mixture was stirred at room temperature for 1 day, and then 2,3-dihydroxynaphthalene (0.26 g, 1.65 mmol) suspended in deoxygenated toluene (40.0 mL) was added to the solution at room

temperature. After stirred the solution at room temperature for 12 hours, the solvent was removed with a vacuum pump. The precipitate was diluted with toluene, then the mixture was filtered, and all volatiles were removed with a rotary evaporator. The obtained residue was diluted with a small amount of chloroform and poured into an excess amount of ethanol at –78 °C. The precipitate was diluted with a small amount of dichloromethane and poured into an excess amount of hexane at room temperature, and then dried in vacuum to afford the titled compound as a pale yellow powder (0.048 g, 7.0%). ^{1}H NMR (CD_2Cl_2): δ 7.33–7.21 (m, 12H), 7.05–7.04 (m, 2H), 6.59 (s, 4H), 6.52 (s, 2H), 5.64 (s, 1H), 2.33 (s, 12H), 2.01 (s, 6H). ^{13}C{^{1}H} NMR (CD_2Cl_2): δ 165.4, 152.5, 137.4, 136.8, 136.6, 135.9, 130.1, 129.6, 128.8, 128.0, 128.0, 126.2, 122.3, 101.9, 99.0, 20.8, 19.4. ^{11}B{^{1}H} NMR (128 MHz, CD_2Cl_2): δ 8.54. HRMS (ESI) $[M+Na]^+$: Found, 649.3001; Calcd., 649.2997.

Synthesis of Mes_FL

A 50 mL two-neck round bottom flask equipped with a stirring bar was charged with 9,9-dimethyl-9*H*-9-ssilafluorene (0.35 g, 1.66 mmol), at room temperature. After the flask was evacuated and refilled with nitrogen, to the flask was added boron tribromide (5.0 mL, 5.0 mmol) at room temperature. The reaction mixture was stirred at 50 °C for 2 days, and then volatiles were removed with a vacuum pump. The residue containing 9-

bromo-9-borafluorene was used for the next reaction without further purification. Another 50 mL two-neck round bottom flask equipped with a stirring bar was charged with **Mes_L** (0.50 g, 1.09 mmol) at room temperature. After the flask was evacuated and refilled with nitrogen, deoxygenated hexane (15.0 mL) was added to the flask at room temperature, and then *n*-butyllithium (0.75 mL, 1.20 mmol) was added at –78 °C. The reaction mixture was stirred at room temperature for 2 hours, and then the solvent was exchanged from hexane to toluene (10 mL). The toluene solution was added slowly at –78 °C for 10 minutes to the solution of precursor 9-bromo-9-borafluorene in toluene (10 mL). After warmed up to room temperature, the mixture was stirred for 40 h. After the reaction solution was quenched with methanol, volatiles were removed with a rotary evaporator. The resulting mixture was purified by silica gel column chromatography with hexane/ethyl acetate = 10/1 as an eluent. Recrystallization from dichloromethane / hexane gave a yellow crystal (0.14 g, 20%).^{1}H NMR (DMSO-d_6, 90 °C): δ 7.39–7.34 (m, 8H), 7.27 (tt, J = 1.24, 1.98 Hz, 2H), 7.22 (m, 4H), 6.98 (ddd, J = 0.82, 6.60 Hz, 2H), 6.71 (t, J = 7.15 Hz, 2H), 6.38 (s, 4H), 5.77 (s, 1H), 1.93 (s, 6H), 1.86 (bs, 12H). ^{13}C{^{1}H} NMR (DMSO-d_6, 90 °C): δ 166.2, 147.8, 140.4, 136.9, 134.0, 133.8, 130.3, 129.1, 127.9, 127.4, 127.2, 126.7 125.1, 117.9, 102.6, 19.5, 19.3. (The signals assigned to the carbons bound to boron were not detected due to the quadrupolar feature of the boron nuclei.) ^{11}B{^{1}H}

NMR (128 MHz, CD_2Cl_2): δ 3.24. HRMS (ESI) $[M+Na]^+$: Found, 643.3261; Calcd., 643.3255.

Synthesis of Ph_FL

A 30 mL Schlenk flask equipped with a stirring bar was charged with 9,9-dimethyl-9*H*-9-ssilafluorene (0.21 g, 1.0 mmol). After the flask was evacuated and refilled with nitrogen, to the flask was added boron tribromide (3.0 mL, 3.0 mmol) at room temperature. The reaction mixture was stirred at 50 °C for 2 days, and then volatiles were removed with a vacuum pump. The residue containing 9-bromo-9-borafluorene was used for the next reaction without further purification. A 30 mL two-neck round bottom flask equipped with a stirring bar was charged with **Ph_L** (0.25 g, 0.67 mmol), at room temperature. After the flask was evacuated and refilled with nitrogen, to the flask was added deoxygenated hexane (15 mL) at room temperature and then *n*-butyllithium (0.50 mL, 0.80 mmol) at –78 °C. The reaction mixture was stirred at room temperature for 2 hours, and then the solvent was exchanged from hexane to deoxygenated toluene (10 mL). The toluene solution was added slowly at –78 °C for 10 minutes to the solution of precursor 9-bromo-9-borafluorene in deoxygenated toluene (5.0 mL). After warmed up

to room temperature, the mixture was stirred for 1 day. After the reaction solution was quenched with methanol, the precipitate was diluted with dichloromethane, then the mixture was filtered, and all volatiles were removed with a rotary evaporator. volatiles were removed with a rotary evaporator. The resulting mixture was purified by silica gel column chromatography with hexane/ethyl acetate = 10/1 as an eluent. Recrystallization from dichloromethane / hexane gave an orange crystal (0.018 g, 5.0%).^{1}H NMR ($CDCl_3$): δ 7.51 (d, *J* = 7.67 Hz, 2H), 7.37 (d, *J* = 7.13 Hz, 2H), 7.36–7.33 (m, 4H), 7.23–7.16 (m, 6H), 7.10 (ddd, *J* = 1.10, 7.40 Hz, 2H), 6.82 (ddd, *J* = 1.10, 7.40 Hz, 2H), 6.73–6.69 (m, 6H), 6.61–6.57 (m, 4H), 5.66 (s, 1H). ^{13}C{^{1}H} NMR ($CDCl_3$): δ 165.7, 148.1, 145.0, 137.9, 131.4, 129.3, 129.0, 127.9, 127.5, 127.1, 127.0, 126.1, 125.1, 118.8, 101.6. (The signals assigned to the carbons bound to boron were not detected due to the quadrupolar feature of the boron nuclei.) ^{11}B{^{1}H} NMR (128 MHz, CD_2Cl_2): δ 3.02. HRMS (ESI) $[M+H]^+$: Found, 537.2504; Calcd., 537.2497.

Synthesis of Ph_FLBr

A 30 mL Schlenk flask equipped with a stirring bar was charged with 4,4'-dibromo-2,2'-diiodobiphenyl (0.22 g, 0.40 mmol), at room temperature. After the flask was evacuated and refilled with nitrogen, to the flask was added deoxygenated Et_2O (7.0 mL) at room temperature and then *n*-butyllithium (0.77 mL, 1.2 mmol) slowly at –78 °C for 7

minutes. After the reaction mixture was stirred at –78 °C for 1.5 h, the solvent was exchanged from Et_2O to deoxygenated hexane (7.0 mL) and then the flask was added boron trichloride (0.50 mL, 0.50 mmol) slowly at –78 °C for 10 minutes. The residue containing 2,7-dibromo-9-chloro-9-borafluorene was used for the next reaction without further purification. A 30 mL two-neck round bottom flask equipped with a stirring bar was charged with **Ph_L** (0.10 g, 0.27 mmol). After the flask was evacuated and refilled with nitrogen, to the flask was added deoxygenated hexane (7.0 mL) at room temperature and then *n*-butyllithium (0.18 mL, 0.29 mmol) at –78 °C. The reaction mixture was stirred at –78 °C for 4 hours, and then the solvent was exchanged from hexane to deoxygenated toluene (7.0 mL). The toluene solution was added slowly at –78 °C for 5 minutes to the solution of precursor 2,7-dibromo-9-chloro-9-borafluorene in deoxygenated toluene (10 mL). After warmed up to room temperature, the mixture was stirred for 20 h. After the reaction solution was quenched with water, the solution was poured into a large amount of chloroform. The combined organic layer was washed with brine, then dried over anhydrous Na_2SO_4. The mixture was filtered, and all volatiles were removed with a rotary evaporator. The residue was purified by silica gel column chromatography with hexane/ethyl acetate = 10/1 as an eluent. Recrystallization from chloroform / hexane gave a yellow crystal (4.3 mg, 2.4%). ^{1}H NMR (CD_2Cl_2): δ 7.53 (d, 2H), 7.37–7.32 (m, 6H),

7.27–7.19 (m, 8H), 6.81–6.77 (m, 6H), 6.61–6.59 (m, 4H), 5.64 (s, 1H). $^{13}C\{^{1}H\}$ NMR (CD_2Cl_2): δ 166.5, 146.1, 144.9, 137.8, 134.5, 130.4, 129.6, 129.6, 128.3, 127.8, 127.8, 125.9, 121.2, 121.1, 101.4. (The signals assigned to the carbons bound to boron were not detected due to the quadrupolar feature of the boron nuclei.) ^{11}B NMR (128 MHz, CD_2Cl_2): δ 2.31. HRMS (ESI) $[M+H]^+$: Found, 693.0725; Calcd., 693.0707.

3. Photophysical Properties

Table S1. Fluorescence lifetimes of the biphenylene complexes[a]

		τ_1 / ns	f_1	τ_2 / ns	f_2	τ_3 / ns	f_3	$\langle\tau\rangle$ / ns[b]
crystal, r.t.	**Mes_FL**	0.27	1	–[c]	–[c]	–[c]	–[c]	0.27
	Ph_FL	0.64	0.31	1.18	0.69	–[c]	–[c]	1.0
	Ph_FLBr	1.59	0.54	4.61	0.46	–[c]	–[c]	3.0
solution, 77 K	**Mes_FL**	0.22	0.35	4.49	0.34	8.47	0.31	4.2
	Ph_FL	5.78	0.59	0.60	0.38	38.3	0.03	4.8
	Ph_FLBr	0.42	0.79	2.54	0.13	8.54	0.08	1.35

[a] $f_i = \alpha_i\tau_i / \Sigma\alpha_i\tau_i$. [b] $\langle\tau\rangle = \Sigma\alpha_i\tau_i^2 / \Sigma\alpha_i\tau_i = \Sigma f_i\tau_i$. [c] Not determined.

Table S2. Phosphorescence lifetimes of the complexes

	τ_{Phos} / ms	
	solution, 77 K	crystal, r.t.
Mes_FL	21.5	–[a]
Ph_FL	30.5	–[a]
Ph_FLBr	63.4	2.1
Mes_cat	117	–[a]
Mes_naph	140	–[a]

[a] Not determined.

Kinetics of Photophysical Processes

Table S3. Rate constants of the biphenylene complexes

	Crystalline state at r.t.		Frozen state at 77 K[a]	
	k_{FL} / 10^7 s^{-1}	k_{nr} / 10^7 s^{-1}	k_{FL} / 10^7 s^{-1}	k_{nr} / 10^7 s^{-1}
Mes_FL	5.7	36	8.3	15
Ph_FL	8.8	5.8	8.6	12
Ph_FLBr	12	0.93	54	20

[a]In 2MeTHF (1×10^{-5} M). [c]k_{FL} and k_{nr} were determined from the following formula: $k_r = \Phi_{PL} / \langle\tau\rangle$ and $k_{nr} = (1 - \Phi_{PL}) / \langle\tau\rangle$.

4. Single Crystal X-ray Analysis

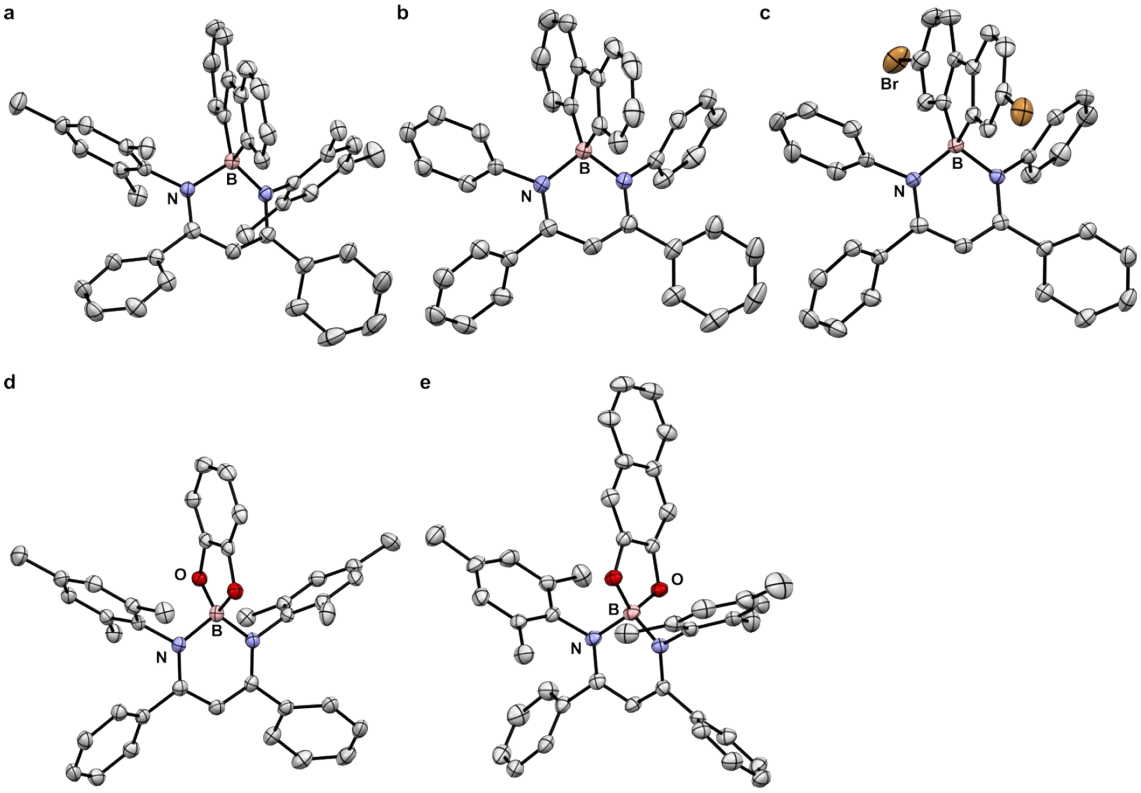

Figure S1. Single crystal X-ray structures of (a) **Mes_FL**, (b) **Ph_FL**, (c) **Ph_FLBr**, (d) **Mes_cat**, and (e) **Mes_naph**. Crystal solvents and hydrogen atoms were omitted for clarity. Legend: white, C; pale pink, B; blue, N; red, O; brown, Br. Ellipsoid: 50% of probability.

Table S4. Selected X-ray data, collection, and refinement parameters for biphenylene complexes

Crystal data	**Mes_FL**	**Ph_FL**	**Ph_FLBr**
CCDC Deposition No.	2529534	2529535	2529536
Chemical formula	$C_{45}H_{41}BN_2 \cdot 0.5\ C_6H_{14}$	$C_{39}H_{29}BN_2$	$C_{39}H_{27}BN_2Br_2 \cdot CHCl_3$
M_r	1325.37	536.45	813.62
Crystal system, Space group	Orthorhombic, $P2_12_12_1$	Orthorhombic, $P2_12_12_1$	Monoclinic, $P2_1/c$
Temperature (K)	150	150	150
a, b, c (Å)	14.271(3), 15.990(3), 33.520(6)	9.777(3), 13.268(4), 22.685(7)	12.034(4), 9.965(3), 29.552(8)
α, β, γ (deg)	90, 90, 90	90, 90, 90	90, 94.320(5), 90
V (Å^3)	7649(2)	2942.8(15)	3533.7(17)
Z	4	4	4
Radiation type	Mo $K\alpha$	Mo $K\alpha$	Mo $K\alpha$
μ (mm^{-1})	0.066	0.070	2.553
Crystal size (mm)	0.27 × 0.27 × 0.19	0.31 × 0.23 × 0.20	0.13 × 0.11 × 0.10
Data collection			
Diffractometer	Rigaku Saturn724+ (4x4 bin mode)		
Absorption correction	Multi-scan REQAB; Rigaku, 1998		
T_{min}, T_{max}	0.863, 1.000	0.856, 1.000	0.770, 1.000
No. of measured, independent, and observed [$I > 2\sigma(I)$] reflections	61077, 17527, 15280	23818, 6613, 5830	27991, 8085, 5892
R_{int}	0.076	0.044	0.051
(sin $\theta/\lambda)_{max}$ (Å^{-1})	0.650	0.648	0.650
Refinement			
$R[F^2 > 2\sigma(F^2)]$, $wR(F^2)$, S	0.054, 0.148, 1.027	0.035, 0.081, 1.01	0.042, 0.11, 1.00
No. of reflections	17527	6613	8085
No. of parameters	933	379	397
H-atom treatment	H atoms treated by a mixture of independent and constrained refinement		
$\Delta\rho_{max}$, $\Delta\rho_{min}$ (e Å^{-3})	0.43, −0.34	0.14, −0.11	0.68, –0.77

Table S5. Solvent masks information for **Ph_FLBr**

Number	*x*	*y*	*z*	Volume	Electron count	Content
1	0.396	0.702	0.885	154.4 Å^3	54.8	$CHCl_3$
2	0.396	0.798	0.385			
3	0.604	0.202	0.615			
4	0.604	0.298	0.115			

Table S6. Selected X-ray data, collection, and refinement parameters for diol complexes

Crystal data	**Mes_cat**	**Mes_naph**
CCDC Deposition No.	2529537	2529538
Chemical formula	$C_{39}H_{37}BN_2O_2$	$C_{43}H_{39}BN_2O_2$
M_r	576.51	626.57
Crystal system, Space group	Monoclinic, $P2_1/c$	Triclinic, P-1
Temperature (K)	150	150
a, b, c (Å)	8.4123(17), 20.137(4), 18.880(4)	11.865(6), 12.187(6), 13.010(6)
α, β, γ (deg)	90, 102.955(3), 90	99.730(5), 99.602(4), 108.243(5)
V (Å^3)	3116.7(11)	1711.6(14)
Z	4	2
Radiation type	Mo $K\alpha$	Mo $K\alpha$
μ (mm^{-1})	0.075	0.074
Crystal size (mm)	0.34 × 0.22 × 0.16	0.25 × 0.12 × 0.07
Data collection		
Diffractometer	Rigaku Saturn724+ (4x4 bin mode)	
Absorption correction	Multi-scan REQAB; Rigaku, 1998	
T_{min}, T_{max}	0.881, 1.000	0.402, 1.000
No. of measured, independent, and observed [$I > 2\sigma(I)$] reflections	24961, 7110, 5752	14025, 7509, 3309
R_{int}	0.040	0.082
$(\sin \theta/\lambda)_{max}$ (Å^{-1})	0.649	0.649
Refinement		
$R[F^2 > 2\sigma(F^2)]$, $\omega R(F^2)$, S	0.041, 0.110, 1.07	0.068, 0.159, 0.92
No. of reflections	7110	7509
No. of parameters	403	439
H-atom treatment	H atoms treated by a mixture of independent and constrained refinement	
$\Delta\rho_{max}$, $\Delta\rho_{min}$ (e Å^{-3})	0.22, −0.20	0.28, −0.30

5. Powder X-Ray Diffraction

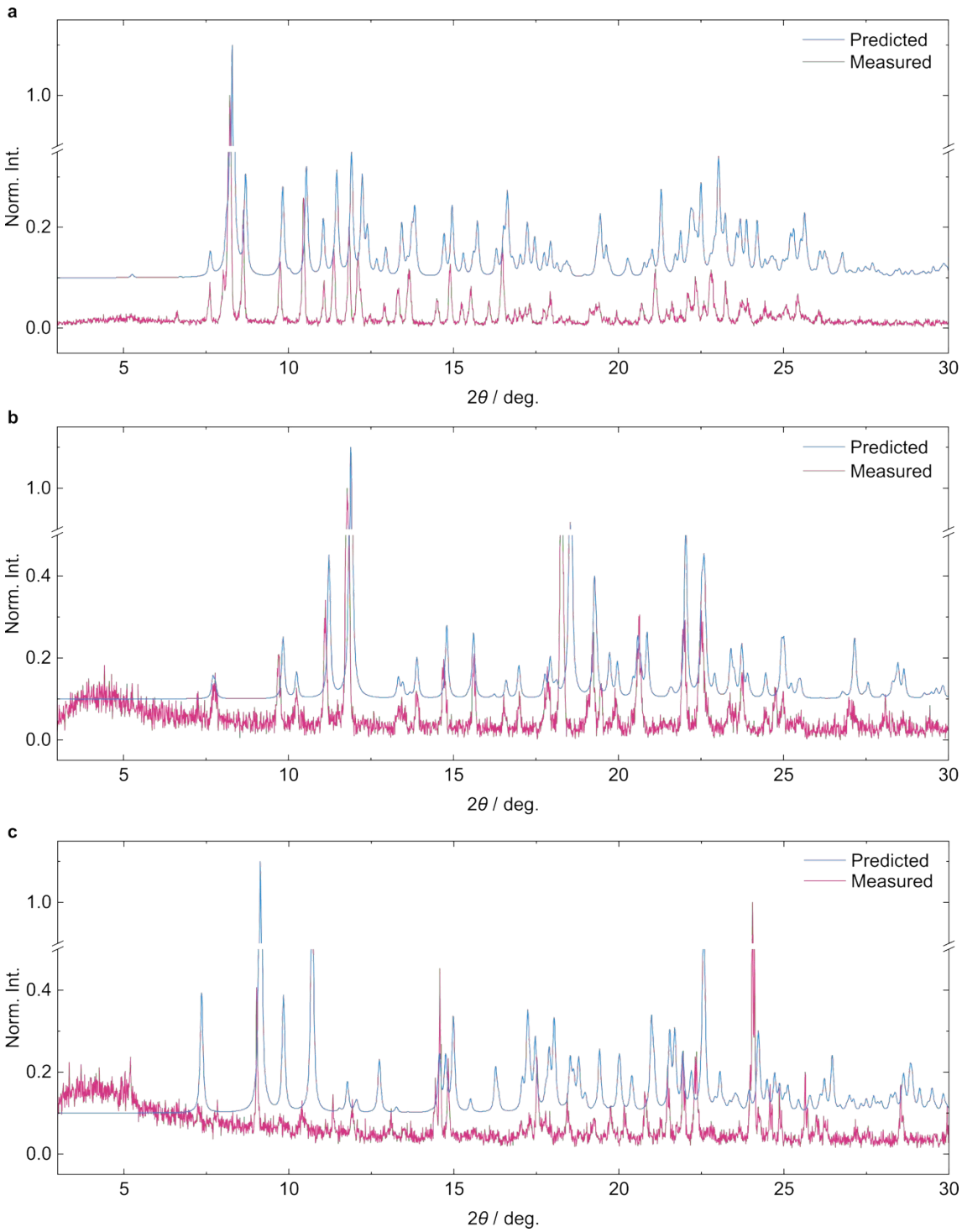

Figure S2. Normalized powder X-ray diffraction patterns of (a) **Mes_FL**, (b) **Ph_FL**, and (c) **Ph_FLBr**. Blue charts show predicted patterns from SCXRD results.

6. DFT Calculations

Geometry optimization and single-point energy calculations were performed on Gaussian 16 Rev. C01.[4] All optimized structures were confirmed as local minima for each potential energy surface (PES) by using frequency calculations. The S_0 structures of the complexes showed good agreement with their single-crystal structures. We assumed that the photophysical properties at the frozen state could be estimated using the S_0 structures because of the restricted molecular motions at cryogenic temperatures. Spin–orbit coupling constants were calculated with Q-Chem 6.[5]

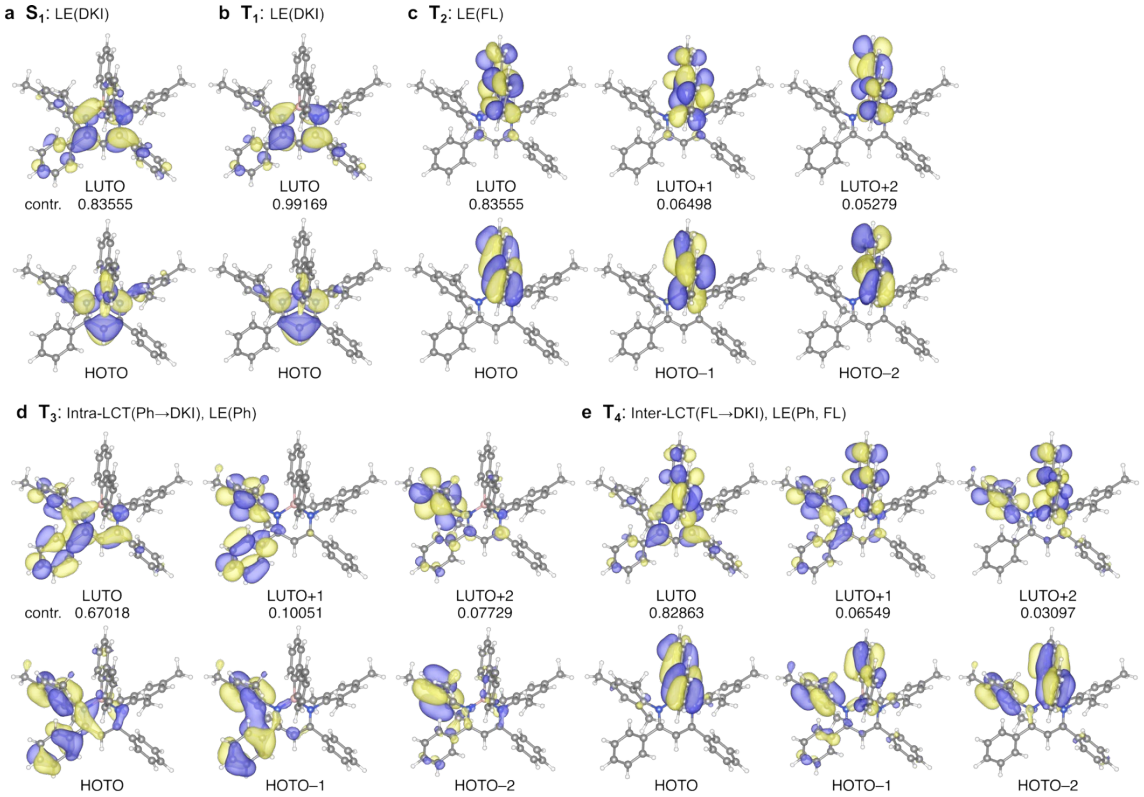

Figure S3. Selected NTOs of **Mes_FL** for (a) S_1, (b) T_1, (c) T_2, (d) T_3, and (e) T_4 states.

Isovalue = 0.03.

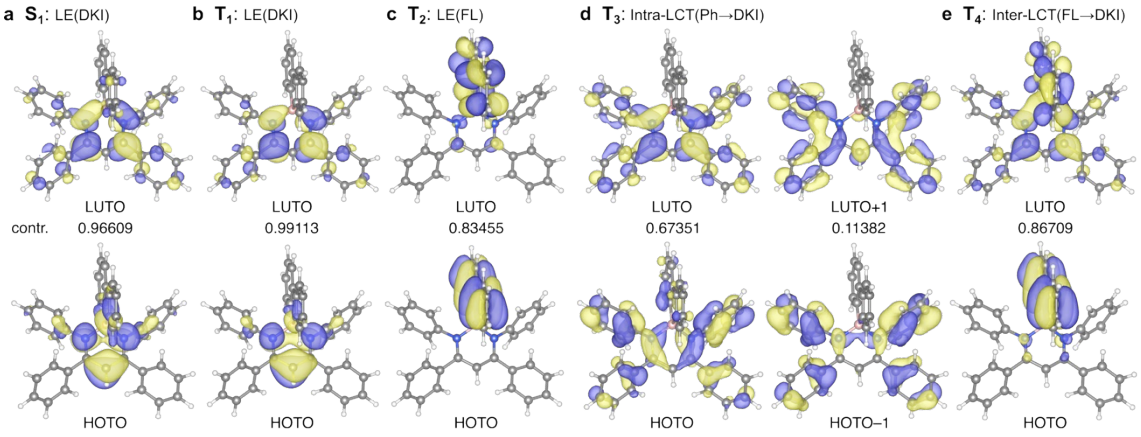

Figure S4. Selected NTOs of **Ph_FL** for (a) S_1, (b) T_1, (c) T_2, (d) T_3, and (e) T_4 states.

Isovalue = 0.03.

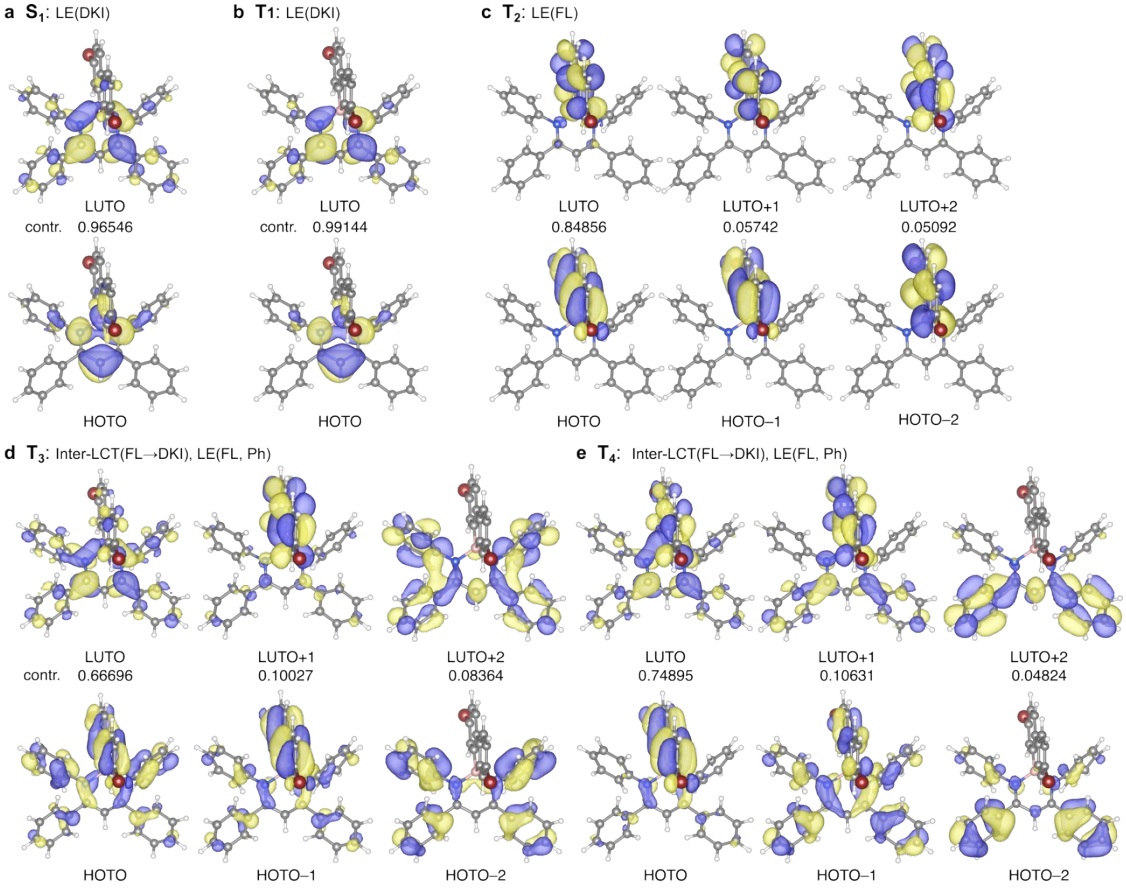

Figure S5. Selected NTOs of **Ph_FLBr** for (a) S_1, (b) T_1, (c) T_2, (d) T_3, and (e) T_4 states.

Isovalue = 0.03.

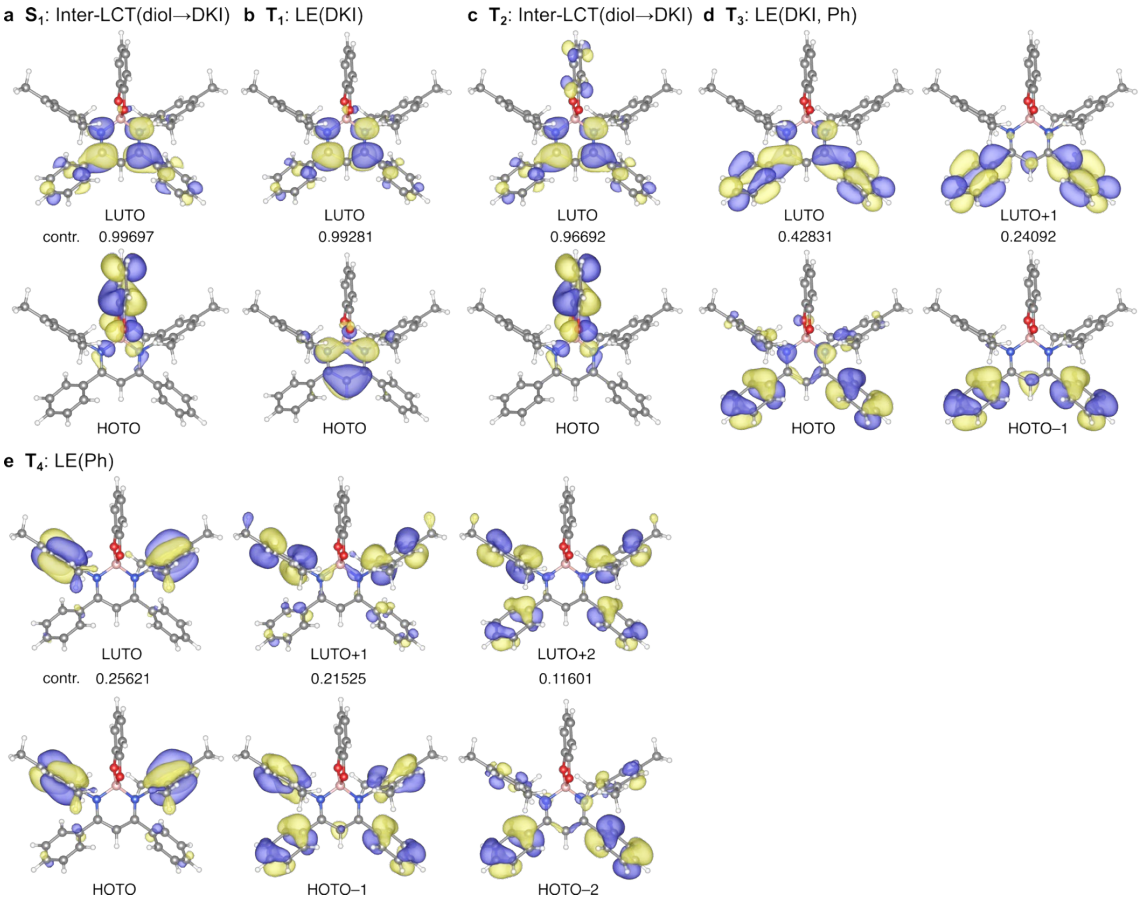

Figure S6. Selected NTOs of **Mes_cat** for (a) S_1, (b) T_1, (c) T_2, (d) T_3, and (e) T_4 states.

Isovalue = 0.03.

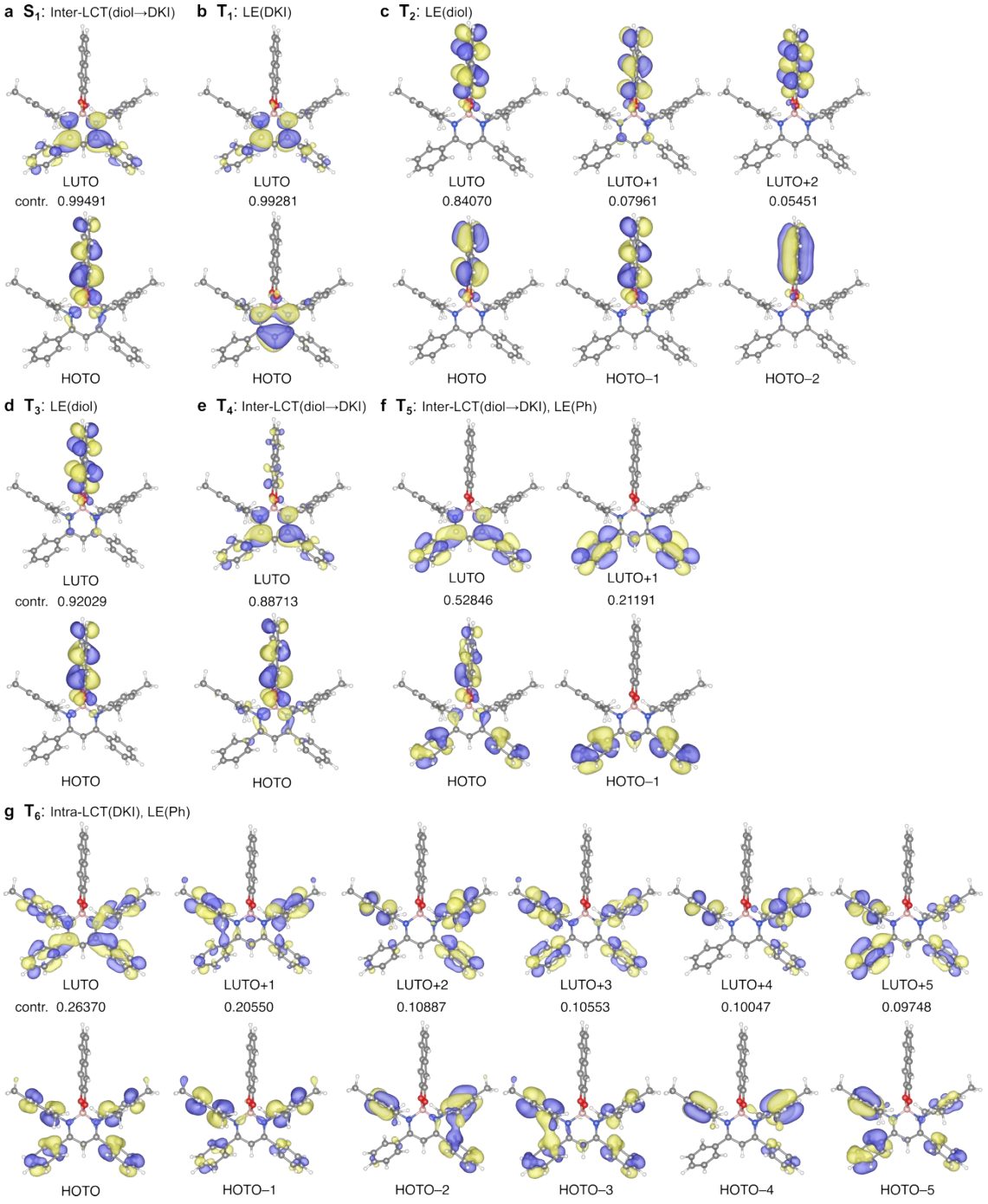

Figure S7. Selected NTOs of **Mes_naph** for (a) S_1, (b) T_1, (c) T_2, (d) T_3, (e) T_4, (f) T_5, and (g) T_6 states. Isovalue = 0.03.6

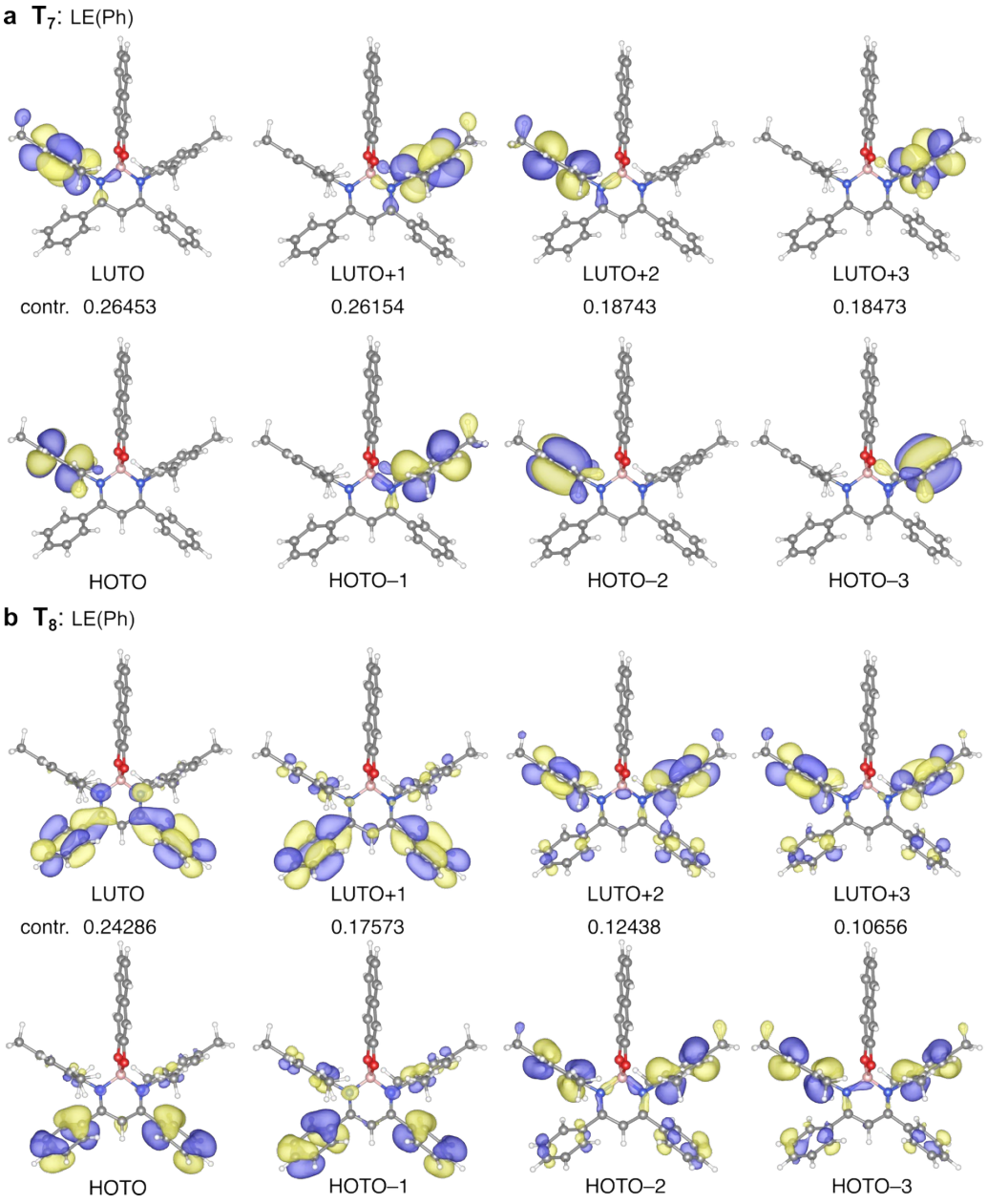

Figure S8. Selected NTOs of **Mes_naph** for (a) T_7 and (b) T_8 states. Isovalue = 0.03.

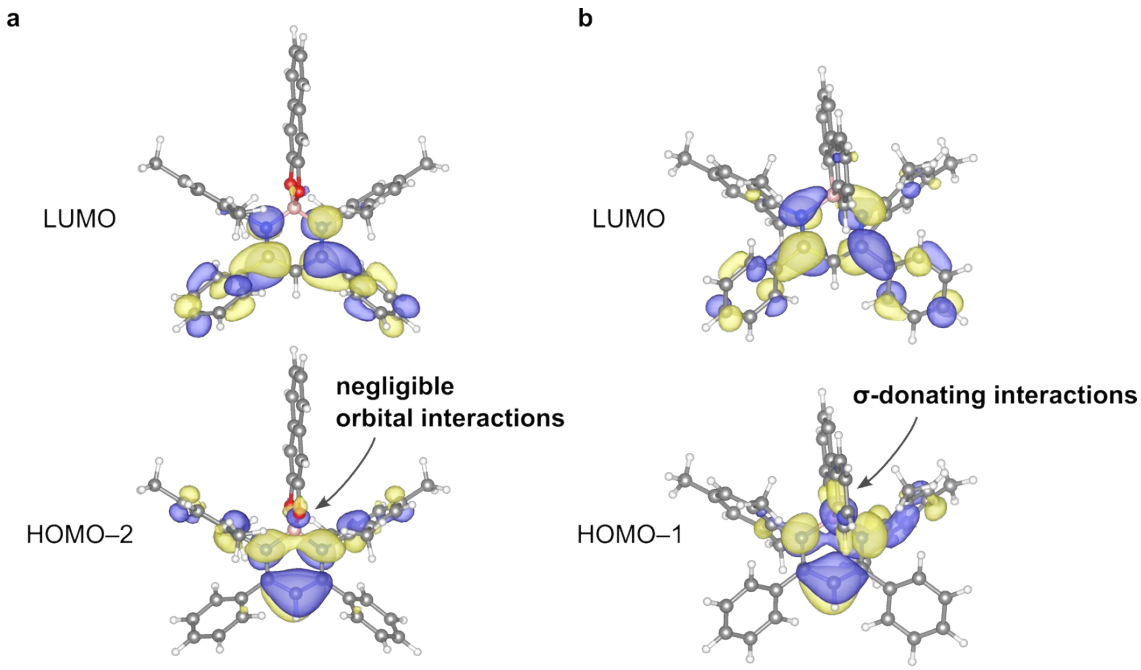

Figure S9. (a) Kohn–Sham HOMO–2 and LUMO of **Mes_naph**. (b) Kohn–Sham HOMO–1 and LUMO of **Mes_FL**. Isovalue = 0.03.

Table S7. Calculated energies of Kohn–Sham orbitals attributed to the DKI unit

	HOMO of DKI / eV[a]	LUMO of DKI / eV[b]	ΔE / eV
Mes_FL	–7.04	–0.87	6.17
Ph_FL	–7.08	–0.98	6.10
Ph_FLBr	–7.32	–1.16	6.17
Mes_cat	–7.47	–0.90	6.58
Mes_naph	–7.60	–0.89	6.71

[a]HOMO–2 of **Mes_naph** and HOMO–1 of the other complexes. [b]LUMO of each molecule.

Table S8. Optimized geometry of **Mes_cat** at the S_0 state

Low Frequencies / cm^{-1}: -2.1833 -1.1121 -0.0007 0.0004 0.0008 0.3638 15.8337 16.6847 25.8571

Center Number	Atomic Number	Coordinates (Angstroms)		
□	□	x	y	z
1	7	1.276192	0.340635	-0.134704
2	7	-1.276126	0.340843	-0.134701
3	6	2.54235	-0.363224	-0.239032
4	6	1.230331	1.67349	0.008791
5	6	-2.542327	-0.362912	-0.239006
6	6	-1.230102	1.673662	0.00871
7	6	2.957205	-0.837164	-1.499627
8	6	3.318573	-0.593706	0.913396
9	6	0.000173	2.332982	0.132974
10	6	-2.957208	-0.836971	-1.499546
11	6	-3.318583	-0.59319	0.913451
12	6	2.150077	-0.600529	-2.754305
13	6	4.162715	-1.539291	-1.582589
14	6	2.920754	-0.079336	2.276529
15	6	4.514401	-1.307569	0.772663
16	1	0.000244	3.411248	0.183855
17	6	-2.150071	-0.600517	-2.754263
18	6	-2.920695	-0.07866	2.276502
19	6	-4.514438	-1.307011	0.772801
20	1	1.285325	-1.268065	-2.78078
21	1	2.760094	-0.781335	-3.643577
22	1	1.759987	0.420824	-2.810492
23	6	4.953101	-1.794456	-0.459074
24	1	4.489921	-1.897398	-2.556182
25	1	3.126408	0.993578	2.369286

26	1	1.857799	-0.238451	2.466649
27	1	3.494071	-0.590045	3.054789
28	1	5.116105	-1.488189	1.66037
29	1	-1.285745	-1.268593	-2.781009
30	1	-2.7603	-0.780746	-3.643512
31	1	-1.759351	0.420599	-2.810259
32	1	-4.489977	-1.897252	-2.555974
33	1	-3.125599	0.994425	2.368889
34	1	-1.857877	-0.238444	2.466856
35	1	-3.494518	-0.588724	3.054809
36	1	-5.116176	-1.48747	1.660519
37	6	-4.162752	-1.53905	-1.582423
38	6	-4.953142	-1.794051	-0.458877
39	6	6.228612	-2.595098	-0.571784
40	1	6.029374	-3.669834	-0.477386
41	1	6.715214	-2.439919	-1.539684
42	1	6.941242	-2.326486	0.21364
43	6	-6.228673	-2.594675	-0.571478
44	1	-6.029472	-3.66939	-0.476765
45	1	-6.941362	-2.325829	0.213815
46	1	-6.715191	-2.439747	-1.53946
47	6	-0.000325	-2.842193	-0.05314
48	6	-0.000293	-2.492211	1.304335
49	6	-0.000545	-4.1641	-0.459064
50	6	-0.000483	-3.454859	2.298227
51	6	-0.00074	-5.150423	0.545113
52	1	-0.000564	-4.424327	-1.512558
53	6	-0.000711	-4.803213	1.894953
54	1	-0.000454	-3.17364	3.346366
55	1	-0.000917	-6.197999	0.258704
56	1	-0.000865	-5.582701	2.651186

57	5	0.000041	-0.557231	0.067561
58	8	-0.000109	-1.718559	-0.82962
59	8	-0.000044	-1.134026	1.437528
60	6	2.453787	2.534299	0.018209
61	6	3.412853	2.504728	-1.005035
62	6	2.6089	3.463734	1.060411
63	6	4.498872	3.378181	-0.980359
64	1	3.30743	1.808996	-1.827387
65	6	3.703588	4.326415	1.089895
66	1	1.872104	3.495397	1.85688
67	6	4.6519	4.287132	0.06747
68	1	5.227505	3.346586	-1.784821
69	1	3.812918	5.028603	1.910986
70	1	5.503262	4.961015	0.08569
71	6	-2.453426	2.534652	0.018029
72	6	-2.608271	3.464444	1.05996
73	6	-3.412643	2.504879	-1.005066
74	6	-3.702834	4.327277	1.089326
75	1	-1.871346	3.496267	1.856304
76	6	-4.498544	3.378482	-0.98051
77	1	-3.307434	1.80886	-1.827197
78	6	-4.651299	4.287788	0.067049
79	1	-3.811947	5.029755	1.910198
80	1	-5.227316	3.346725	-1.78484
81	1	-5.502571	4.961787	0.085161

Table S9. Optimized geometry of **Mes_naph** at the S_0 state

Low Frequencies / cm^{-1}: -1.2678 -0.0007 -0.0005 -0.0003 0.9009 1.7666 4.8876 15.9147 17.8480

Center Number	Atomic Number	Coordinates (Angstroms)		
□	□	x	y	z
1	8	0.721252	-0.423786	-1.242548
2	8	0.874599	-0.313952	1.078105
3	7	-0.32194	1.52948	-0.081178
4	7	-1.367808	-0.776622	0.061956
5	6	1.915017	-0.918502	-0.844277
6	6	-2.665489	1.190135	-0.209954
7	1	-3.645976	1.630243	-0.304358
8	6	-3.831956	-0.972631	-0.114559
9	6	0.82891	2.390363	0.089521
10	6	-2.558031	-0.194941	-0.081349
11	6	2.922619	-1.418433	-1.605903
12	1	2.837219	-1.47681	-2.685676
13	6	2.011595	-0.846204	0.572685
14	6	-1.553104	2.030241	-0.167271
15	6	-1.81319	3.499369	-0.193657
16	6	1.134263	2.84954	1.381454
17	6	-1.239799	-2.21466	0.166644
18	6	-4.7045	-0.767436	-1.186921
19	1	-4.416388	-0.089809	-1.983704
20	6	4.103732	-1.879563	-0.946915
21	6	1.644457	2.708158	-0.999427
22	6	3.116349	-1.272534	1.236573
23	1	3.184406	-1.209367	2.317168
24	6	-1.040223	-2.79935	1.423196
25	6	2.25832	3.646119	1.552978

26	1	2.495395	4.00643	2.550525
27	6	-4.214502	-1.838872	0.910868
28	1	-3.562071	-1.997602	1.759094
29	6	4.200608	-1.805891	0.473804
30	6	-2.695895	4.038613	0.745242
31	1	-3.137718	3.388994	1.493565
32	6	-5.922612	-1.431906	-1.245625
33	1	-6.582529	-1.271492	-2.0917
34	6	5.19261	-2.413205	-1.673676
35	1	5.114995	-2.468539	-2.756041
36	6	-1.277194	-2.994813	-0.998204
37	6	-2.99985	5.393917	0.732983
38	1	-3.67691	5.800328	1.476958
39	6	2.763198	3.512662	-0.772978
40	1	3.394635	3.770699	-1.619369
41	6	-1.005638	-1.997554	2.698634
42	1	0.005867	-1.641025	2.900433
43	1	-1.334816	-2.609557	3.542017
44	1	-1.639813	-1.110023	2.647486
45	6	-6.293629	-2.29464	-0.221827
46	1	-7.246806	-2.811466	-0.262685
47	6	5.382124	-2.268521	1.097203
48	1	5.452655	-2.210485	2.179888
49	6	-1.261092	4.337951	-1.163238
50	1	-0.596216	3.932124	-1.914321
51	6	0.278648	2.487425	2.56452
52	1	-0.731508	2.897864	2.475227
53	1	0.714613	2.88146	3.484658
54	1	0.196661	1.402351	2.656084
55	6	6.326858	-2.854655	-1.039126
56	1	7.150811	-3.260775	-1.617248

57	6	-5.439509	-2.490141	0.857254
58	1	-5.726348	-3.155396	1.664813
59	6	6.422895	-2.781218	0.363727
60	1	7.320729	-3.130719	0.863523
61	6	3.090979	3.986928	0.488252
62	6	-1.506153	-2.387736	-2.3562
63	1	-2.52815	-2.009174	-2.455437
64	1	-1.356735	-3.13738	-3.13581
65	1	-0.817645	-1.559672	-2.531062
66	6	-2.441904	6.222285	-0.232576
67	1	-2.681731	7.280402	-0.247627
68	6	1.371526	2.241454	-2.406615
69	1	2.05266	1.431306	-2.678924
70	1	1.530168	3.061315	-3.113696
71	1	0.361828	1.853884	-2.531915
72	6	-1.578913	5.689055	-1.183304
73	1	-1.148615	6.32837	-1.946937
74	6	-0.881834	-4.182127	1.490491
75	1	-0.736869	-4.641751	2.464737
76	6	-1.109585	-4.370786	-0.875408
77	1	-1.138669	-4.980012	-1.774745
78	6	-0.902827	-4.984333	0.356043
79	6	4.321236	4.825384	0.712299
80	1	4.122233	5.64914	1.403141
81	1	4.691092	5.249324	-0.223936
82	1	5.129591	4.226648	1.144883
83	5	-0.021729	0.001622	-0.042438
84	6	-0.684762	-6.470891	0.452149
85	1	-0.982116	-6.855762	1.430569
86	1	0.371963	-6.72057	0.309447
87	1	-1.252349	-7.008041	-0.311821

Table S10. Optimized geometry of **Mes_FL** at the S_0 state

Low Frequencies / cm^{-1}: -2.2798 -1.9885 -0.7794 -0.0007 -0.0005 0.0007 14.1797 20.4739 29.8918

Center Number	Atomic Number	Coordinates (Angstroms)		
□	□	x	y	z
1	6	-1.344051	1.532877	0.436002
2	6	-0.14196	2.212967	0.678406
3	6	1.113459	1.672367	0.333041
4	1	-0.183764	3.238536	1.015343
5	7	-1.330137	0.222393	0.127995
6	7	1.241972	0.361846	0.099775
7	6	0.06361	-0.968903	2.104966
8	6	0.104284	-2.077142	-0.132236
9	6	-0.014301	-0.20596	3.273413
10	6	0.245417	-2.368255	2.235488
11	6	0.068299	-2.544944	-1.446341
12	6	0.275731	-3.023649	0.908351
13	6	0.093463	-0.809277	4.535008
14	1	-0.158228	0.870113	3.217037
15	6	0.354022	-2.976326	3.487832
16	6	0.21154	-3.909057	-1.72859
17	1	-0.084291	-1.854559	-2.271869
18	6	0.422807	-4.386101	0.635204
19	6	0.279853	-2.188475	4.640542
20	1	0.030775	-0.20173	5.434279
21	1	0.491291	-4.051467	3.57561
22	6	0.392693	-4.824914	-0.690725
23	1	0.179606	-4.25691	-2.757751
24	1	0.555759	-5.104371	1.440535

25	1	0.362867	-2.652704	5.619733
26	1	0.50522	-5.882805	-0.913206
27	5	-0.002422	-0.594474	0.512664
28	6	-2.433833	-0.359218	-0.609555
29	6	-3.226765	-1.378445	-0.034654
30	6	-2.712122	0.083379	-1.922836
31	6	-4.248689	-1.950158	-0.797234
32	6	-3.740945	-0.532638	-2.644746
33	6	-4.516472	-1.559224	-2.110191
34	1	-4.858509	-2.726484	-0.339937
35	1	-3.938782	-0.188223	-3.657749
36	6	2.449367	-0.166394	-0.514835
37	6	2.635349	-0.024031	-1.908125
38	6	3.419598	-0.833392	0.258275
39	6	3.779381	-0.562613	-2.49979
40	6	4.551243	-1.351204	-0.385939
41	6	4.750775	-1.240508	-1.75962
42	1	3.912362	-0.446742	-3.573026
43	1	5.301412	-1.854247	0.220616
44	6	-1.983858	1.225481	-2.593785
45	1	-1.019378	1.439603	-2.138141
46	1	-1.819902	1.00667	-3.65355
47	1	-2.579664	2.144502	-2.541019
48	6	-3.053912	-1.865146	1.383722
49	1	-2.417926	-2.754389	1.418973
50	1	-2.586122	-1.123444	2.031745
51	1	-4.025506	-2.138387	1.807198
52	6	1.634193	0.687158	-2.781924
53	1	1.946677	0.650116	-3.82864
54	1	0.646386	0.227365	-2.710909
55	1	1.524226	1.741613	-2.508105

56	6	3.334721	-1.003656	1.757125
57	1	2.643949	-0.305636	2.228691
58	1	2.984859	-2.006726	2.018659
59	1	4.325955	-0.87672	2.205328
60	6	-5.597193	-2.233068	-2.92096
61	1	-5.226583	-3.155471	-3.385328
62	1	-6.453058	-2.508374	-2.296632
63	1	-5.958346	-1.585196	-3.725071
64	6	5.961477	-1.844435	-2.429727
65	1	5.732556	-2.835757	-2.840303
66	1	6.311656	-1.223698	-3.260505
67	1	6.789394	-1.9671	-1.72536
68	6	-2.612153	2.31734	0.516287
69	6	-3.722872	1.8223	1.218306
70	6	-2.686248	3.606747	-0.034942
71	6	-4.873397	2.594526	1.359616
72	1	-3.675589	0.839713	1.671292
73	6	-3.842767	4.374151	0.097061
74	1	-1.835725	4.00031	-0.581986
75	6	-4.940183	3.8701	0.795582
76	1	-5.718968	2.19941	1.914641
77	1	-3.885144	5.365	-0.345519
78	1	-5.840717	4.467625	0.90255
79	6	2.248337	2.638622	0.198901
80	6	3.45564	2.474199	0.894653
81	6	2.077445	3.789271	-0.587954
82	6	4.464596	3.43028	0.796074
83	1	3.59708	1.610997	1.531891
84	6	3.094358	4.736725	-0.699168
85	1	1.143412	3.931903	-1.122306
86	6	4.291705	4.559714	-0.005909

87	1	5.388514	3.291858	1.349597
88	1	2.948197	5.61331	-1.323344
89	1	5.083467	5.298753	-0.085584

Table S11. Optimized geometry of **Ph_FL** at the S_0 state

Low Frequencies / cm^{-1}: -0.9929 -0.5172 -0.0005 0.0002 0.0006 2.3346 16.7388 20.3033 37.4813

Center Number	Atomic Number	Coordinates (Angstroms)		
□	□	x	y	z
1	7	1.261835	0.231173	-0.142582
2	7	-1.26211	0.23052	-0.142699
3	6	-2.440658	-0.375565	-0.68806
4	6	2.925578	0.030971	-1.9293
5	1	2.409595	0.814811	-2.473734
6	6	0.000871	-2.583029	1.779448
7	6	-2.457539	2.372395	0.128865
8	6	2.440644	-0.37419	-0.688027
9	6	0.000472	-2.096052	-0.549901
10	6	0.001125	-3.131691	0.402852
11	6	0.000211	-1.17289	1.756774
12	6	3.53277	2.012457	0.943299
13	1	3.486572	1.094634	1.518556
14	6	3.082058	-1.399018	0.004346
15	1	2.692513	-1.719927	0.963937
16	6	-4.209976	-2.003716	-0.538321
17	1	-4.702662	-2.802432	0.006713
18	6	0.000708	-2.434218	-1.898372
19	1	0.000122	-1.6563	-2.658437
20	6	-0.000128	-0.492013	2.971929
21	1	-0.000588	0.595175	2.991152
22	6	-3.081431	-1.400701	0.004417
23	1	-2.691628	-1.721399	0.963977
24	6	4.058187	-0.570842	-2.466844

25	1	4.429586	-0.247517	-3.434065
26	6	1.219959	1.540347	0.098068
27	6	4.210874	-2.001441	-0.538494
28	1	4.703995	-2.799934	0.006477
29	6	4.654375	2.827856	1.025411
30	1	5.480735	2.540515	1.667319
31	6	0.002072	-4.469073	0.018102
32	1	0.002647	-5.263468	0.759417
33	6	-2.925844	0.029266	-1.929341
34	1	-2.410246	0.813303	-2.47385
35	6	0.001631	-3.772415	-2.295534
36	1	0.001829	-4.026306	-3.351437
37	6	4.705238	-1.588491	-1.772945
38	1	5.585869	-2.062162	-2.194453
39	6	0.001172	-3.288776	2.979305
40	1	0.001639	-4.375325	2.987279
41	6	-3.534127	2.010635	0.943059
42	1	-3.487603	1.092796	1.51826
43	6	-1.221023	1.539737	0.097912
44	6	2.45607	2.373651	0.128978
45	6	4.719996	4.006482	0.286553
46	1	5.600604	4.637997	0.346208
47	6	2.521406	3.564799	-0.596131
48	1	1.687053	3.851284	-1.228226
49	6	-0.000701	2.177369	0.34613
50	1	-0.000958	3.212633	0.653365
51	6	0.002333	-4.785465	-1.33925
52	1	0.00311	-5.825468	-1.651971
53	6	-2.523412	3.563571	-0.596171
54	1	-1.689184	3.850498	-1.228231
55	6	-4.704656	-1.591084	-1.772751

56	1	-5.585077	-2.065267	-2.194128
57	6	-4.058181	-0.573161	-2.466785
58	1	-4.429807	-0.250109	-3.43401
59	6	3.651615	4.372766	-0.525774
60	1	3.695686	5.289561	-1.104864
61	6	0.000176	-1.192351	4.181506
62	1	-0.000122	-0.650844	5.123066
63	6	0.00082	-2.585192	4.183348
64	1	0.001017	-3.125832	5.125216
65	6	-4.656121	2.825512	1.025184
66	1	-5.48239	2.537711	1.667007
67	6	-4.722264	4.004165	0.286419
68	1	-5.603145	4.635296	0.346152
69	6	-3.654007	4.370992	-0.525836
70	1	-3.698478	5.287784	-1.104897
71	5	-0.000103	-0.668623	0.208153

Table S12. Optimized geometry of **Ph_FLBr** complexes at the S_0 state

Low Frequencies / cm^{-1}:	-0.0084	-0.0024	-0.0007	1.3131	2.0980	2.2782
	11.5084	13.7074	20.5133			

Center Number	Atomic Number	Coordinates (Angstroms)		
□	□	x	y	z
1	35	4.328624	0.000013	3.64647
2	35	-5.677132	-0.000019	-0.092637
3	6	1.862029	2.458236	-2.095413
4	6	-1.621476	-0.000006	0.765686
5	6	1.291728	-1.220381	-1.493671
6	6	1.862049	-2.458218	-2.095417
7	6	2.214981	3.54012	-1.284372
8	1	2.032097	3.493799	-0.216706
9	6	-0.227004	0.000002	2.687896
10	6	-0.597039	2.426551	-0.611546
11	6	0.700972	0.000002	1.62738
12	6	1.291719	1.220394	-1.493668
13	6	-2.837544	-0.000011	0.098121
14	1	-2.882735	-0.000013	-0.986081
15	6	2.118698	2.522053	-3.466203
16	1	1.848857	1.68336	-4.099872
17	6	-0.597015	-2.426558	-0.611549
18	6	-1.613062	-0.000002	2.171436
19	6	2.059289	0.000005	1.922709
20	1	2.805315	0.000006	1.134671
21	6	2.470535	0.000008	3.253652
22	6	2.215003	-3.540101	-1.284376
23	1	2.032112	-3.493784	-0.216711
24	6	1.906401	0.000009	-1.794817

25	1	2.828865	0.000014	-2.356339
26	6	-1.277216	2.869873	-1.742931
27	1	-1.151558	2.342253	-2.682614
28	6	2.118726	-2.522029	-3.466206
29	1	1.848883	-1.683336	-4.099874
30	6	-0.772856	3.082678	0.604671
31	1	-0.249048	2.726619	1.484894
32	6	-1.277204	-2.869875	-1.742929
33	1	-1.151567	-2.342242	-2.682608
34	6	-2.798837	-0.000004	2.897607
35	1	-2.793616	-0.000001	3.983771
36	6	2.809498	4.666553	-1.838586
37	1	3.087695	5.496731	-1.197682
38	6	0.193725	0.000005	4.013281
39	1	-0.522177	0.000005	4.830223
40	6	2.698836	3.657234	-4.022513
41	1	2.880834	3.700895	-5.091457
42	6	-0.772804	-3.082704	0.604662
43	1	-0.248986	-2.726651	1.484881
44	6	2.809529	-4.666529	-1.83859
45	1	3.087727	-5.496708	-1.197687
46	6	1.557534	0.000008	4.30017
47	1	1.905383	0.00001	5.326859
48	6	-1.619611	4.182201	0.682358
49	1	-1.755716	4.685759	1.634006
50	6	-2.120209	3.972958	-1.661957
51	1	-2.649297	4.309977	-2.547483
52	6	3.046756	4.731111	-3.209244
53	1	3.504381	5.61534	-3.641071
54	6	-4.016131	-0.000009	2.220829
55	1	-4.951936	-0.000011	2.767994

56	6	3.046795	-4.731083	-3.209247
57	1	3.504427	-5.615308	-3.641073
58	6	-4.01928	-0.000013	0.831564
59	6	2.698873	-3.657206	-4.022515
60	1	2.880877	-3.700863	-5.091458
61	6	-2.294881	4.631896	-0.449155
62	1	-2.95938	5.487157	-0.383861
63	5	-0.103717	-0.000001	0.210629
64	6	-2.120183	-3.972971	-1.661956
65	1	-2.649281	-4.309985	-2.547477
66	6	-1.619545	-4.182238	0.682349
67	1	-1.755629	-4.685809	1.633992
68	6	-2.294828	-4.631926	-0.449159
69	1	-2.959317	-5.487196	-0.383866
70	7	0.234823	-1.260742	-0.683199
71	7	0.234812	1.260744	-0.683196

7. NMR Charts

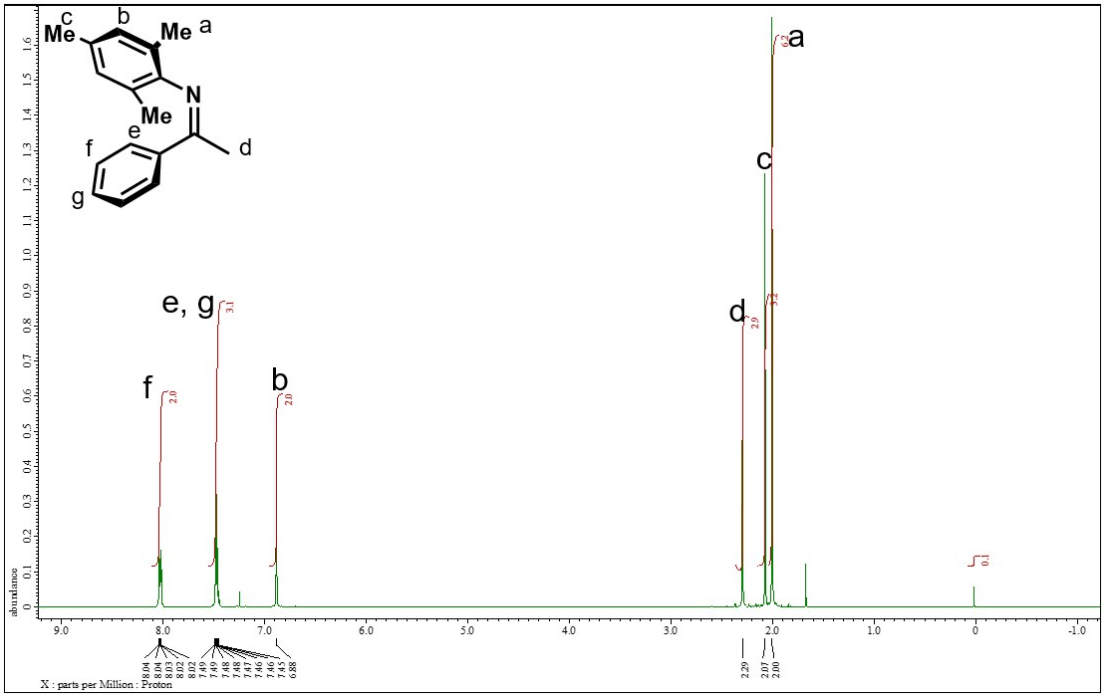

Chart S1. ^{1}H NMR spectrum of **Mes_imine** in $CDCl_3$.

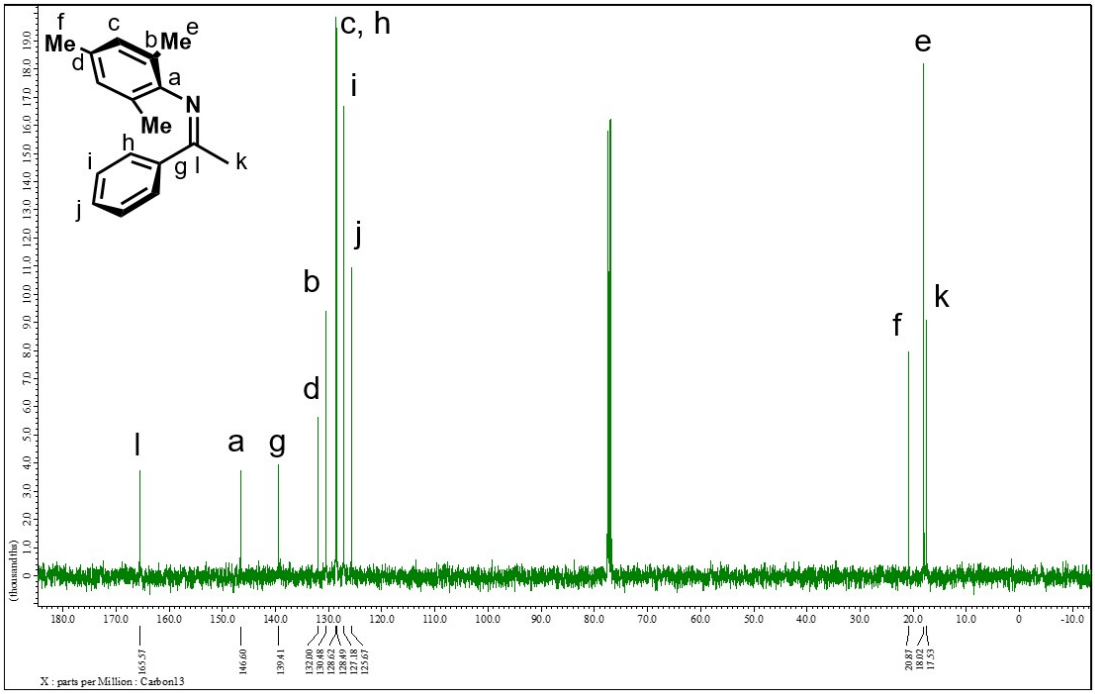

Chart S2. $^{13}C\{^{1}H\}$ NMR spectrum of **Mes_imine** in $CDCl_3$.

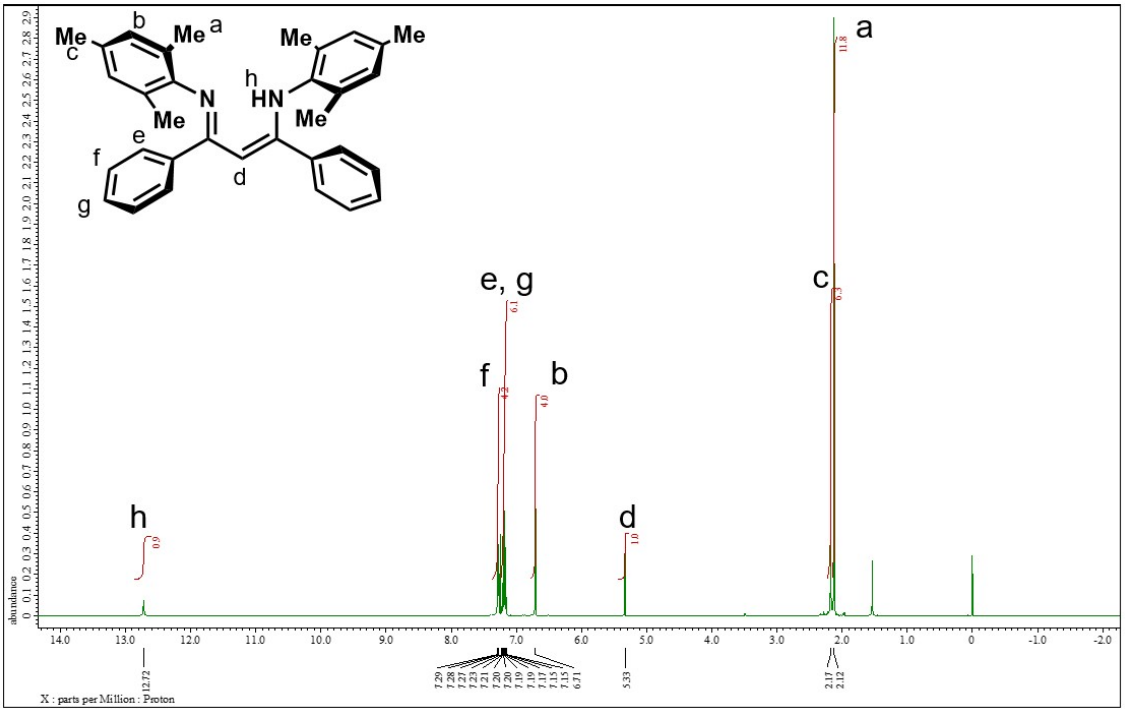

Chart S3. ^{1}H NMR spectrum of **Mes_L** in $CDCl_3$.

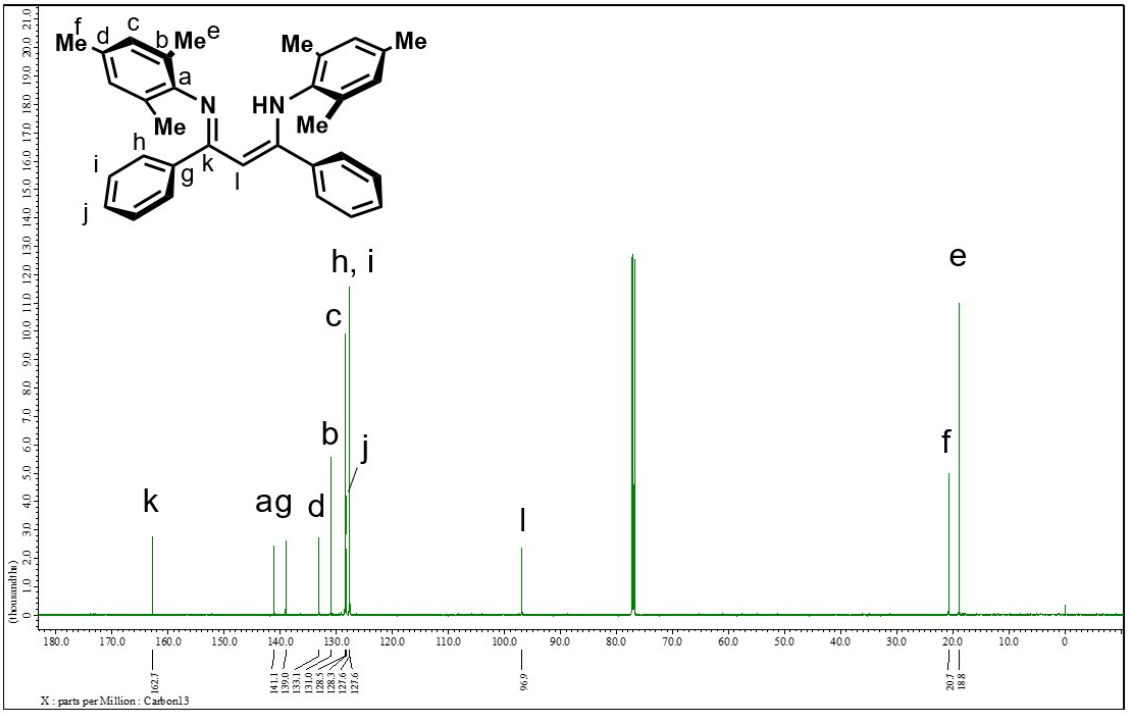

Chart S4. ^{13}C{^{1}H} NMR spectrum of **Mes_L** in $CDCl_3$.

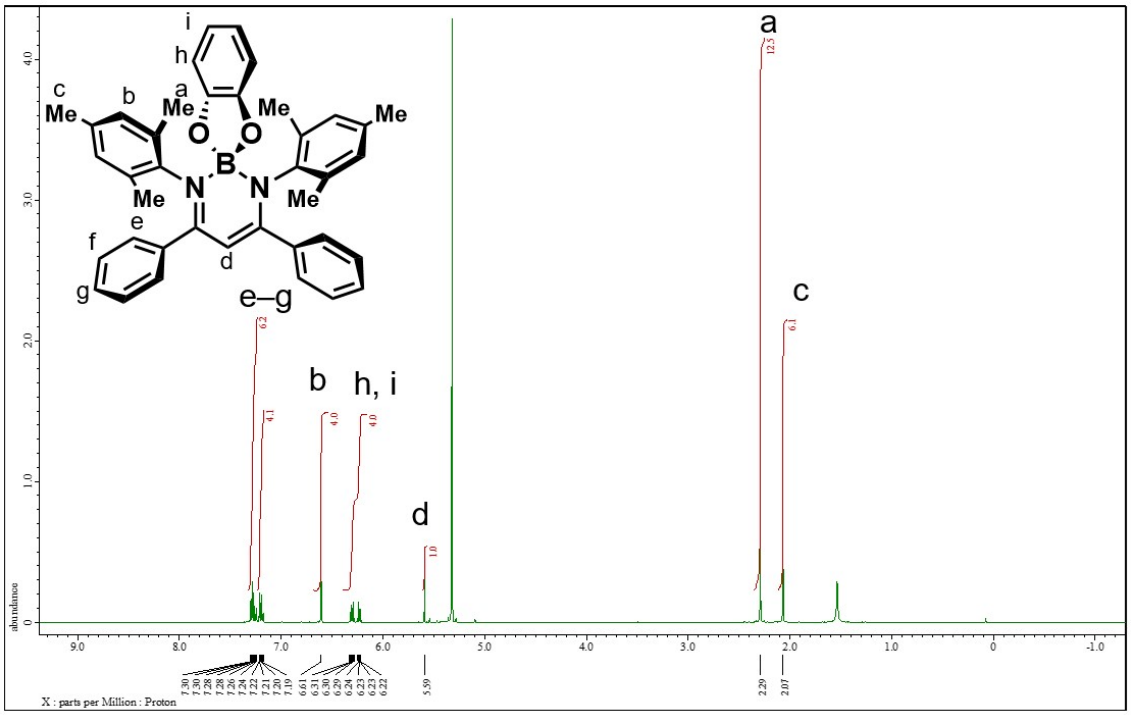

Chart S5. ^{1}H NMR spectrum of **Mes_cat** in CD_2Cl_2.

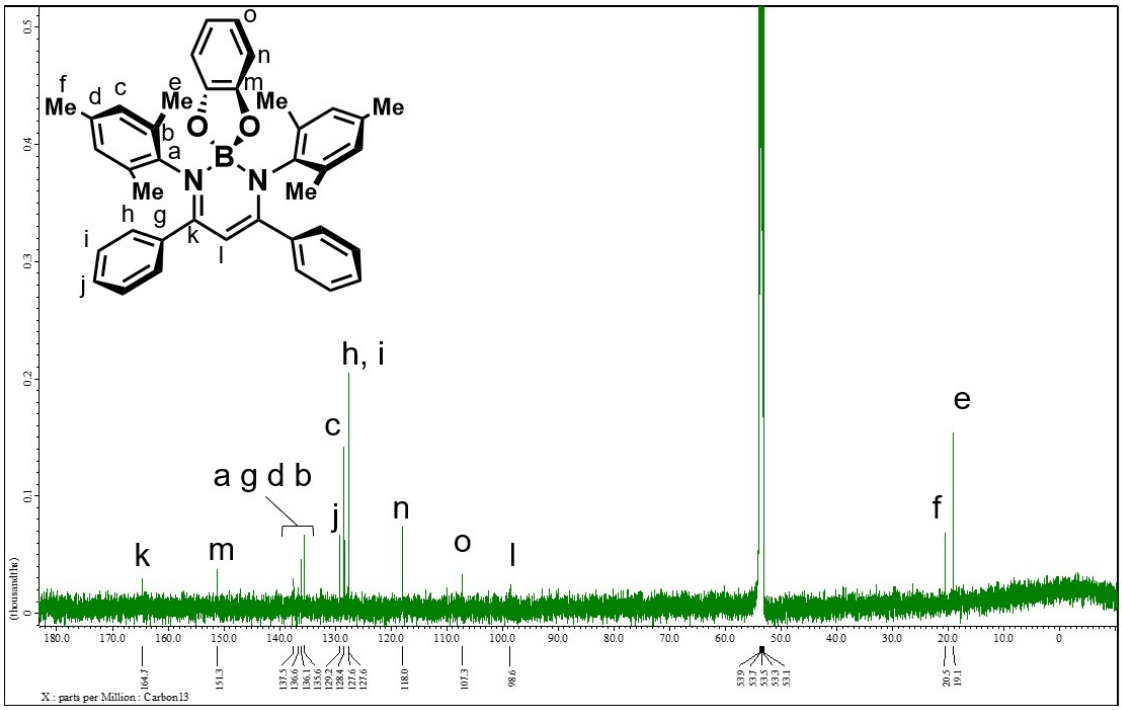

Chart S6. $^{13}C\{^{1}H\}$ NMR spectrum of **Mes_cat** in CD_2Cl_2.

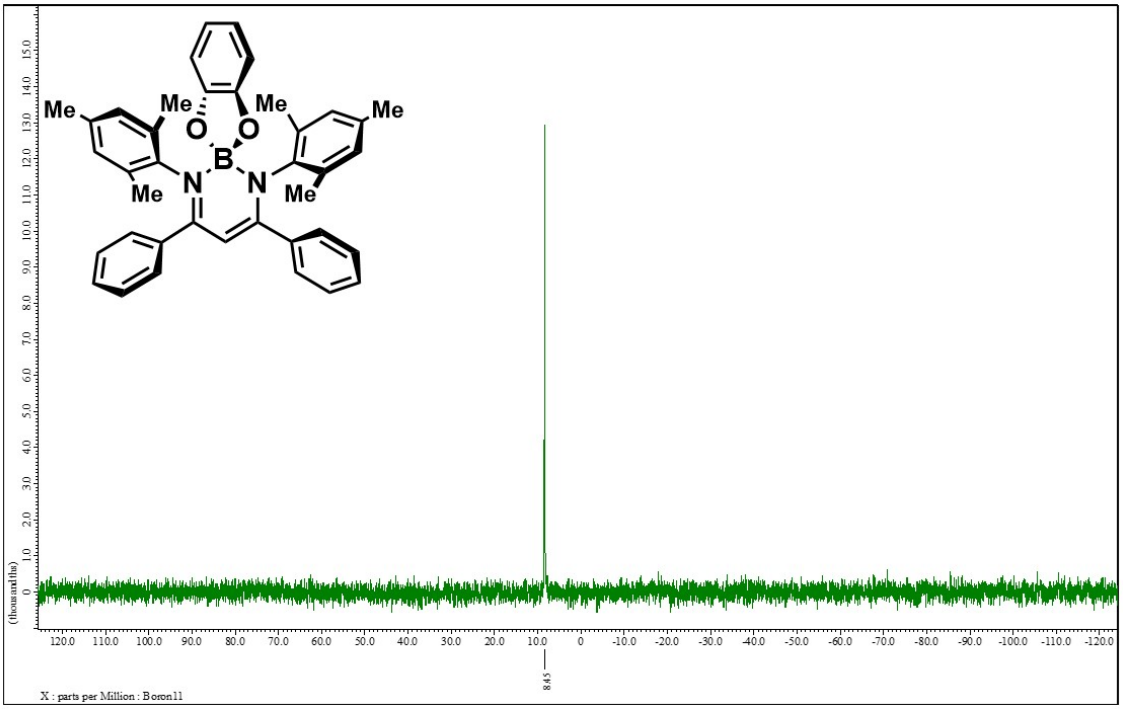

Chart S7. $^{11}B\{^{1}H\}$ NMR spectrum of **Mes_cat** in CD_2Cl_2.

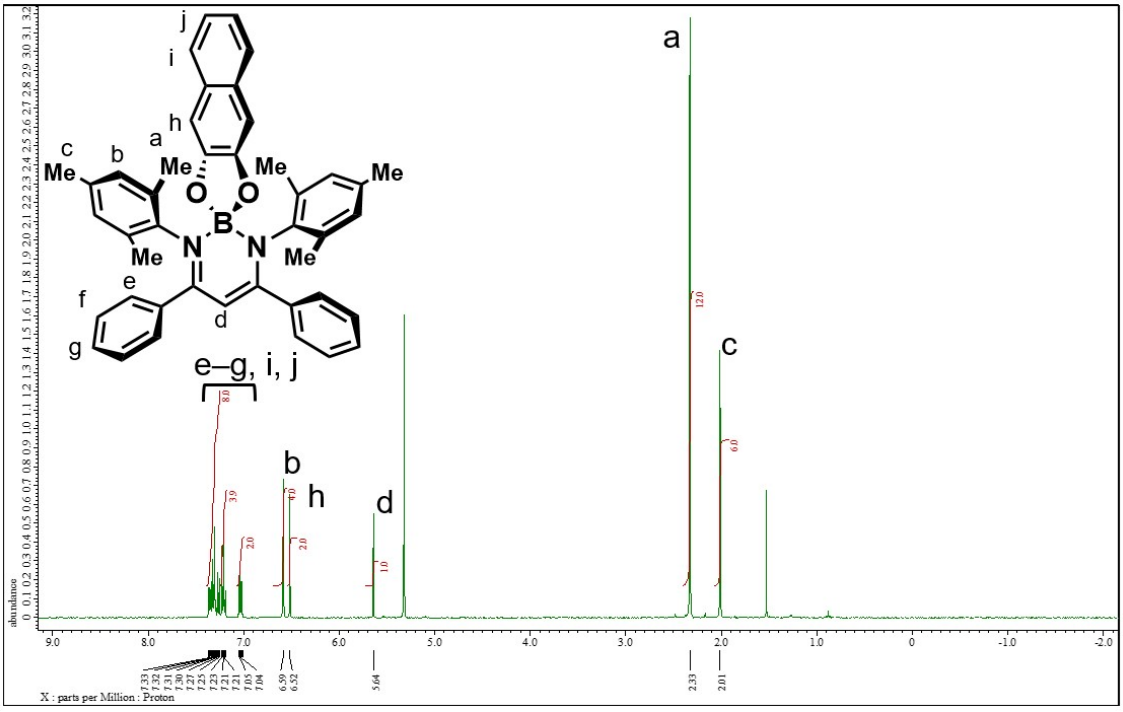

Chart S8. ^{1}H NMR spectrum of **Mes_naph** in CD_2Cl_2.

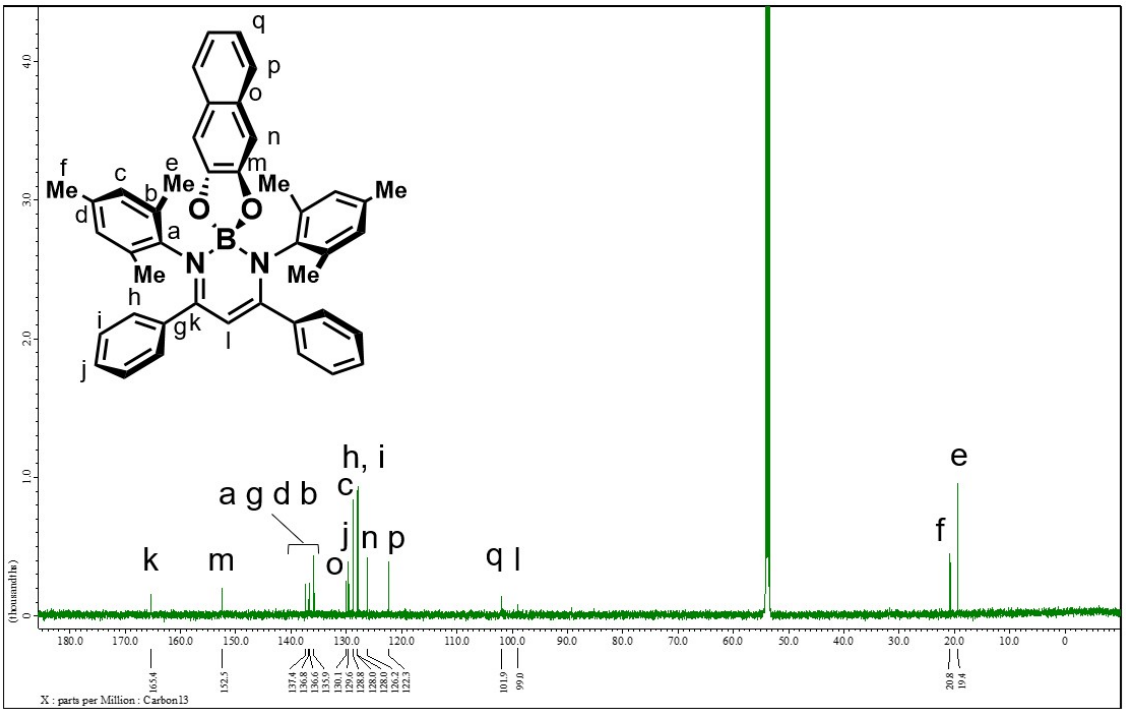

Chart S9. $^{13}C\{^{1}H\}$ NMR spectrum of **Mes_naph** in CD_2Cl_2.

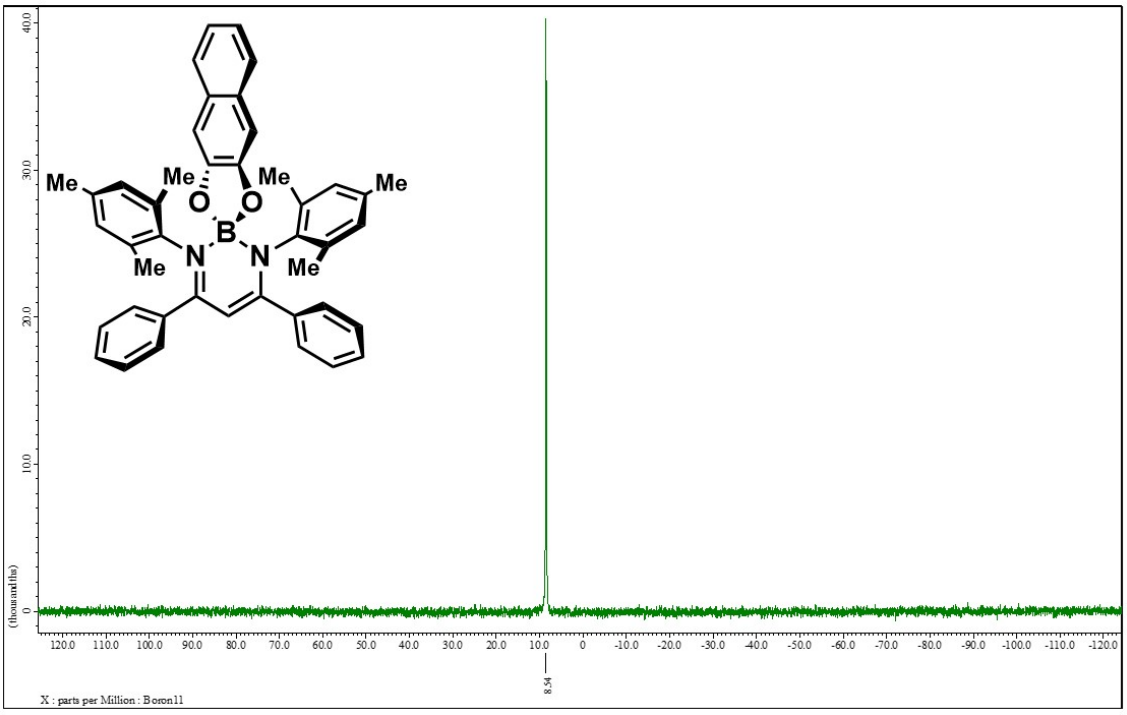

Chart S10. $^{11}B\{^{1}H\}$ NMR spectrum of **Mes_naph** in CD_2Cl_2.

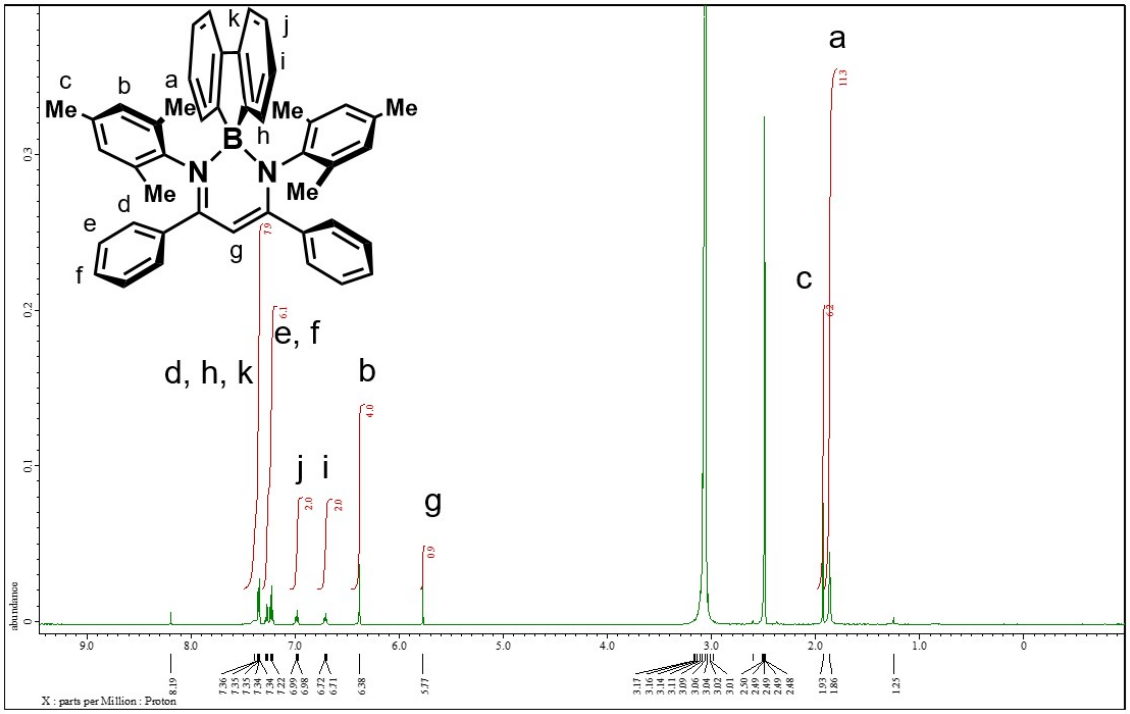

Chart S11. ^{1}H NMR spectrum of **Mes_FL** in DMSO-d_6 at 363 K.

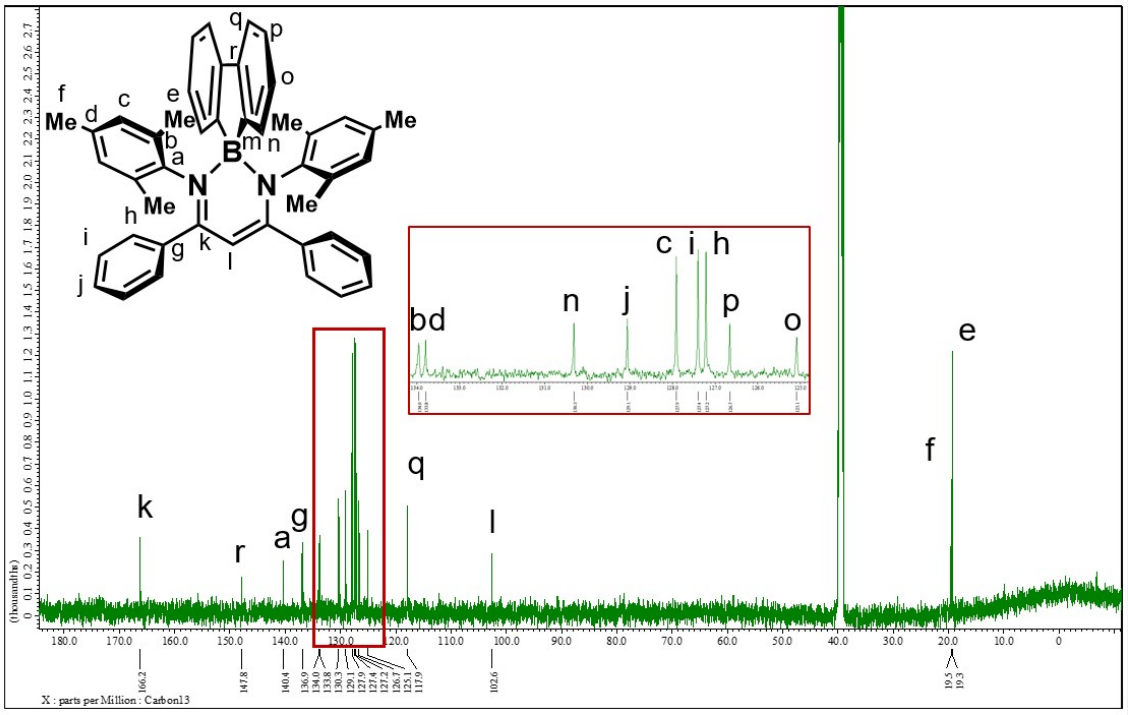

Chart S12. $^{13}C\{^{1}H\}$ NMR spectrum of **Mes_FL** in DMSO-d_6 at 363 K.

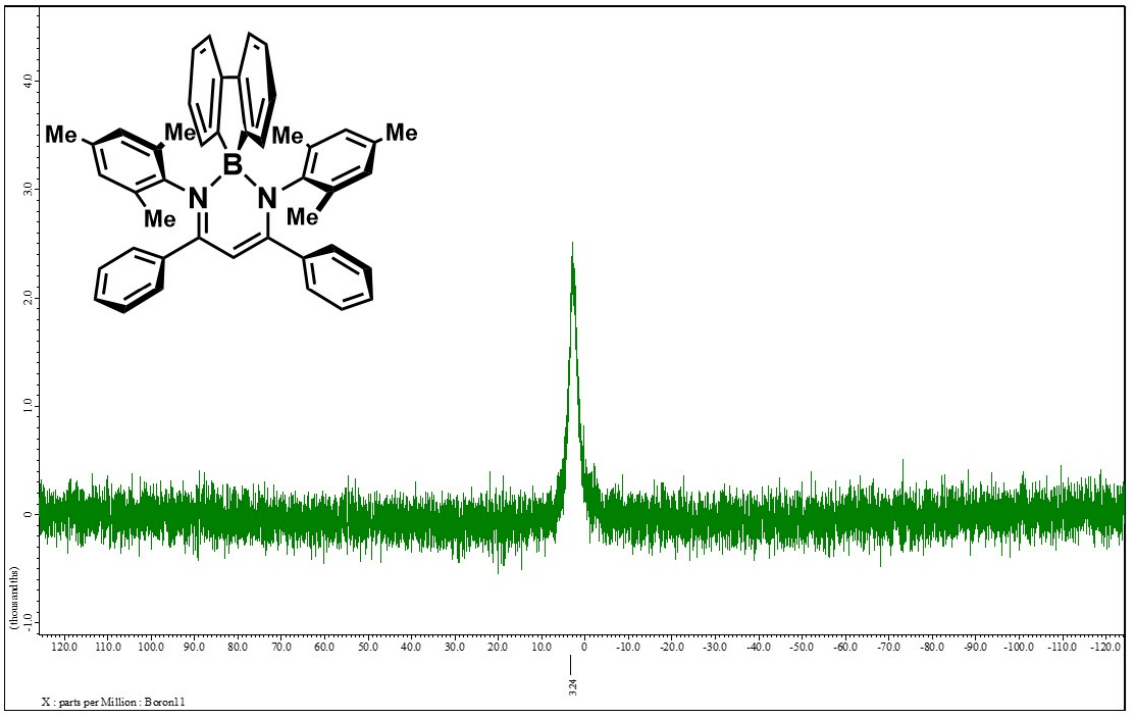

Chart S13. $^{11}B\{^{1}H\}$ NMR spectrum of **Mes_FL** in $CDCl_3$.

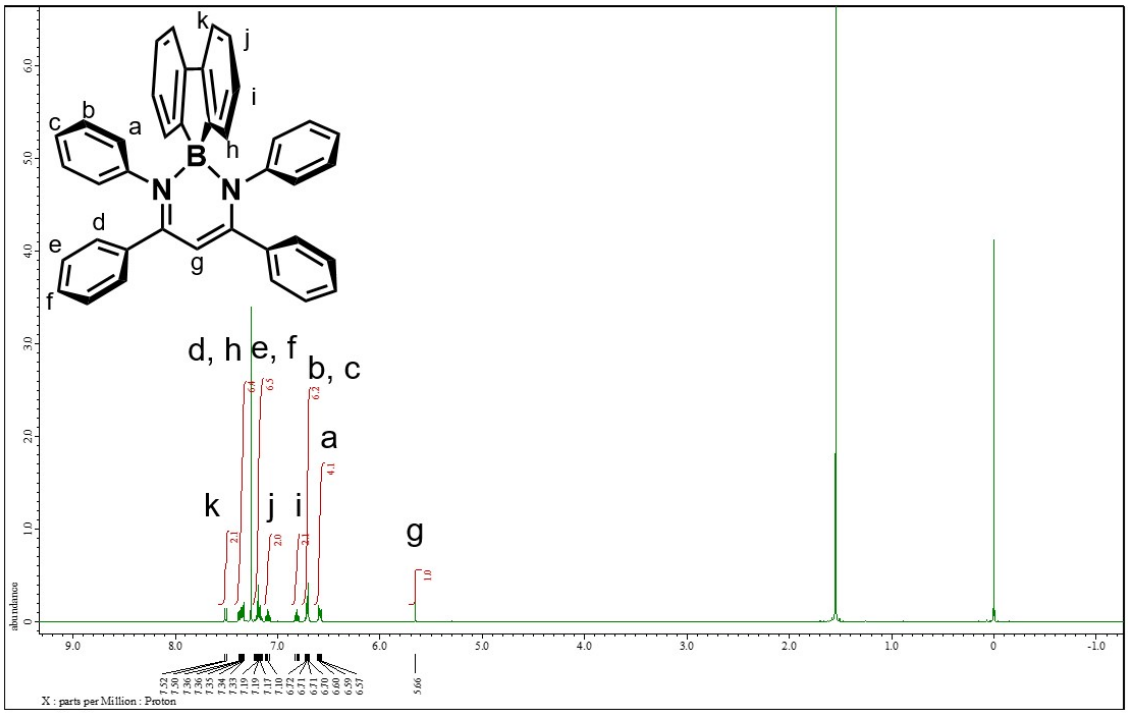

Chart S14. ^{1}H NMR spectrum of **Ph_FL** in $CDCl_3$.

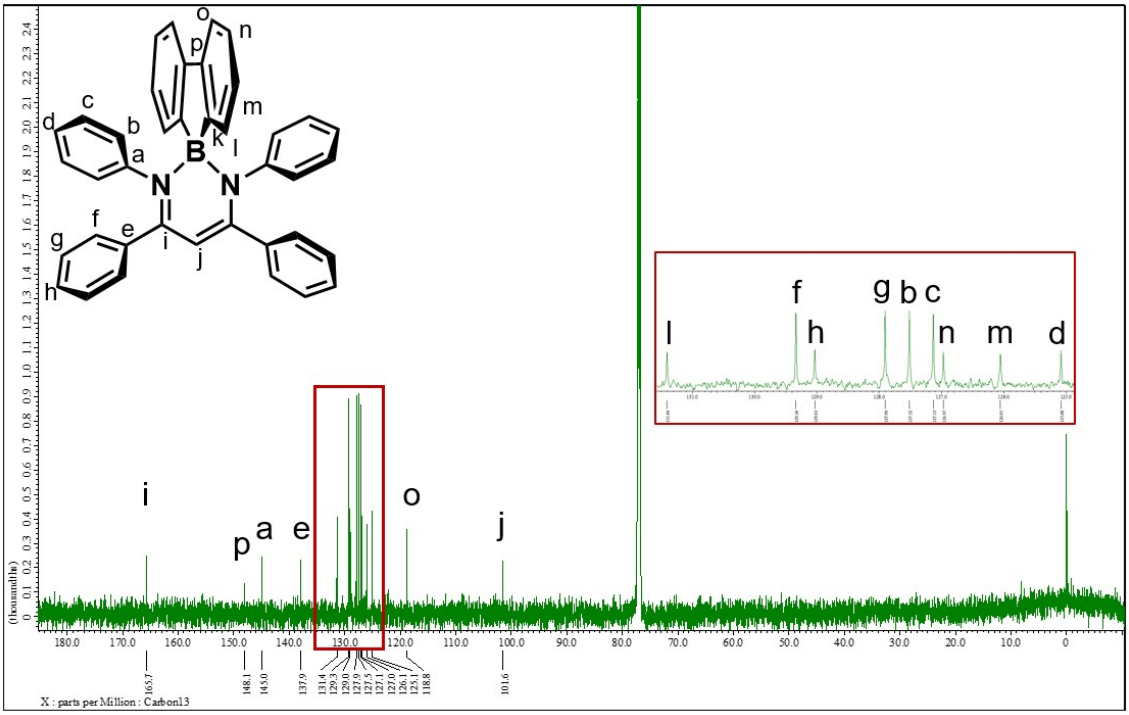

Chart S15. $^{13}C\{^{1}H\}$ NMR spectrum of **Ph_FL** in $CDCl_3$.

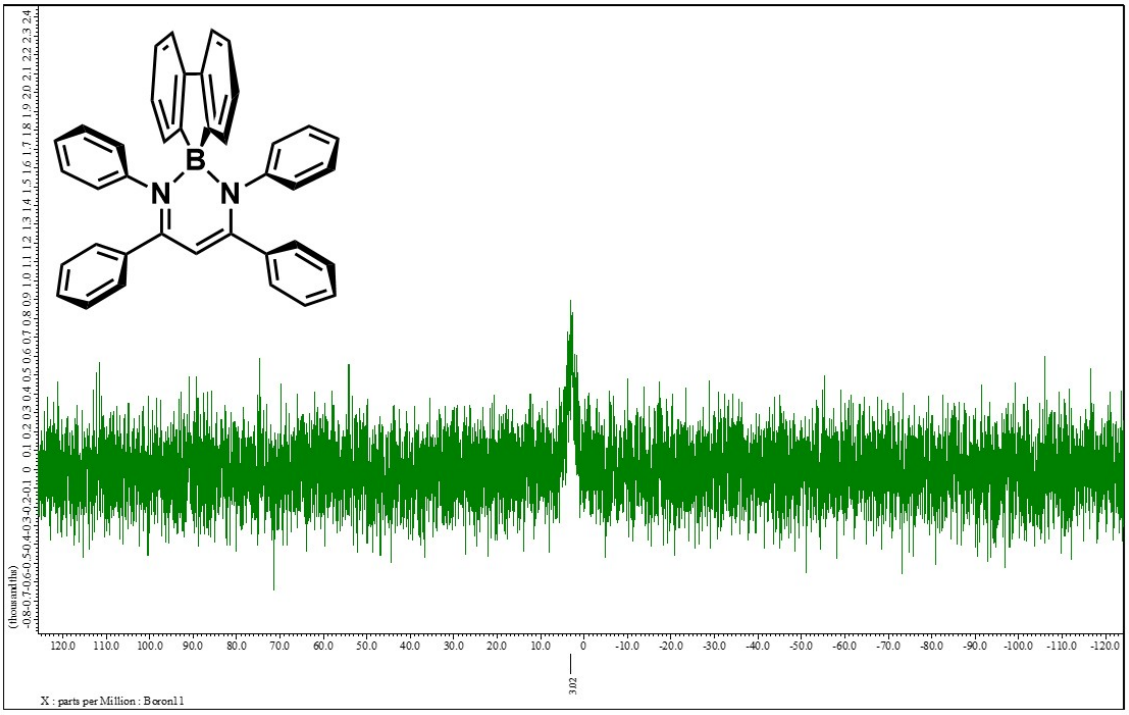

Chart S16. $^{11}B\{^{1}H\}$ NMR spectrum of **Ph_FL** in $CDCl_3$.

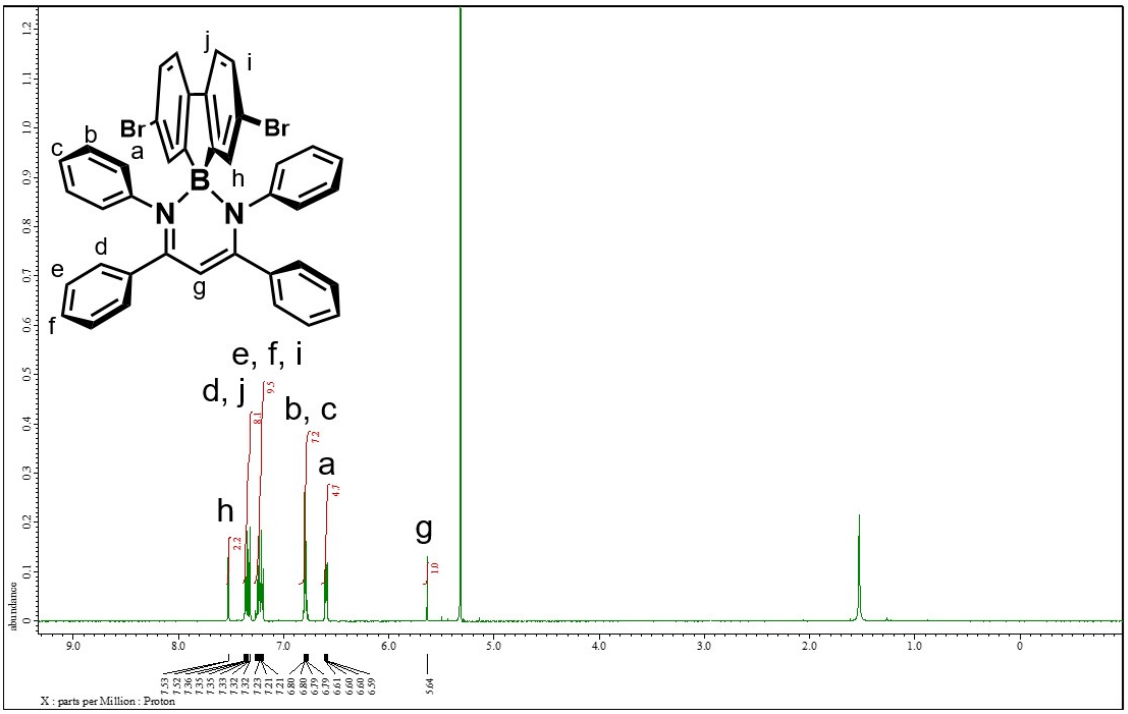

Chart S17. ^{1}H NMR spectrum of **Ph_FLBr** in CD_2Cl_2.

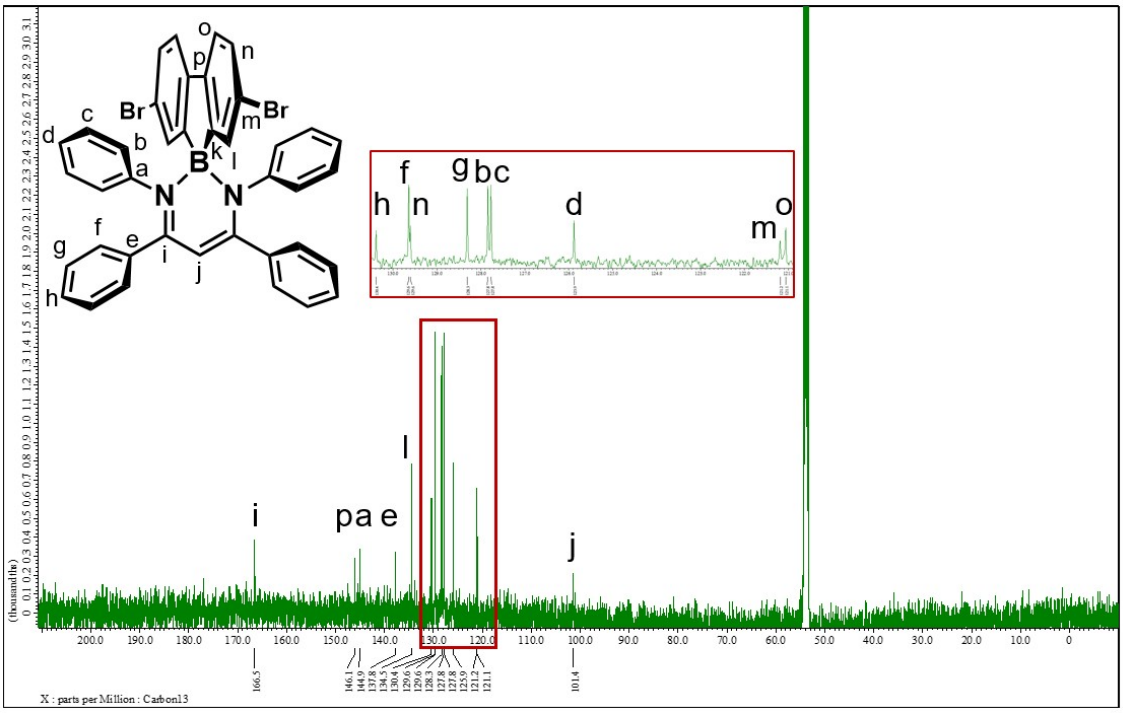

Chart S18. $^{13}C\{^{1}H\}$ NMR spectrum of **Ph_FLBr** in CD_2Cl_2.

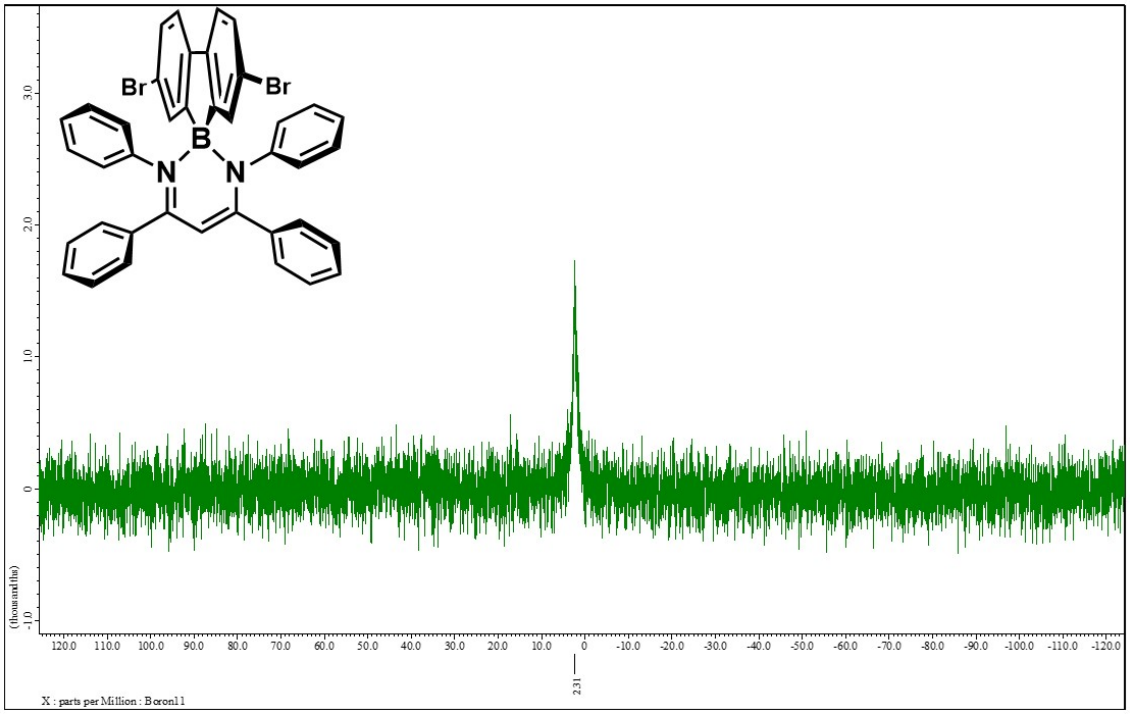

Chart S19. $^{11}B\{^{1}H\}$ NMR spectrum of **Ph_FLBr** in CD_2Cl_2.

8. References

1 R. Yoshii, A. Hirose, K. Tanaka and Y. Chujo, *Chem. Eur. J.*, 2014, **20**, 8320–8324.

2 R. Yoshii, A. Hirose, K. Tanaka and Y. Chujo, *J. Am. Chem. Soc.*, 2014, **136**, 18131–18139.

3 T. van Dijk, S. Burck, M. K. Rong, A. J. Rosenthal, M. Nieger, C. J. Slootweg and K. Lammertsma, *Angew. Chem. Int. Ed.*, 2014, **53**, 9068–9071.

4 M. J. Frisch, G. W. Trucks, H. B. Schlegel, G. E. Scuseria, M. A. Robb, J. R. Cheeseman, G. Scalmani, V. Barone, G. A. Petersson, H. Nakatsuji, X. Li, M. Caricato, A. V. Marenich, J. Bloino, B. G. Janesko, R. Gomperts, B. Mennucci, H. P. Hratchian, J. V. Ortiz, A. F. Izmaylov, J. L. Sonnenberg, D. Williams-Young, F. Ding, F. Lipparini, F. Egidi, J. Goings, B. Peng, A. Petrone, T. Henderson, D. Ranasinghe, V. G. Zakrzewski, J. Gao, N. Rega, G. Zheng, W. Liang, M. Hada, M. Ehara, K. Toyota, R. Fukuda, J. Hasegawa, M. Ishida, T. Nakajima, Y. Honda, O. Kitao, H. Nakai, T. Vreven, K. Throssell, J. A. Montgomery, Jr., J. E. Peralta, F. Ogliaro, M. J. Bearpark, J. J. Heyd, E. N. Brothers, K. N. Kudin, V. N. Staroverov, T. A. Keith, R. Kobayashi, J. Normand, K. Raghavachari, A. P. Rendell, J. C. Burant, S. S. Iyengar, J. Tomasi, M. Cossi, J. M. Millam, M. Klene, C. Adamo, R. Cammi, J. W. Ochterski, R. L. Martin, K. Morokuma, O. Farkas, J. B. Foresman and D. J. Fox, *Gaussian 16 Rev. C.01*, Wallingford, CT, 2016.

5 E. Epifanovsky, A. T. B. Gilbert, X. Feng, J. Lee, Y. Mao, N. Mardirossian, P. Pokhilko, A. F. White, M. P. Coons, A. L. Dempwolff, Z. Gan, D. Hait, P. R. Horn, L. D. Jacobson, I. Kaliman, J. Kussmann, A. W. Lange, K. U. Lao, D. S. Levine, J. Liu, S. C. McKenzie, A. F. Morrison, K. D. Nanda, F. Plasser, D. R. Rehn, M. L. Vidal, Z.-Q. You, Y. Zhu, B. Alam, B. J. Albrecht, A. Aldossary, E. Alguire, J. H. Andersen, V. Athavale, D. Barton, K. Begam, A. Behn, N. Bellonzi, Y. A. Bernard, E. J. Berquist, H. G. A. Burton, A. Carreras, K. Carter-Fenk, R. Chakraborty, A. D. Chien, K. D. Closser, V. Cofer-Shabica, S. Dasgupta, M. de Wergifosse, J. Deng, M. Diedenhofen, H. Do, S. Ehlert, P.-T. Fang, S. Fatehi, Q. Feng, T. Friedhoff, J. Gayvert, Q. Ge, G. Gidofalvi, M. Goldey, J. Gomes, C. E. González-Espinoza, S. Gulania, A. O. Gunina, M. W. D. Hanson-Heine, P. H. P. Harbach, A. Hauser, M. F. Herbst, M. H. Vera, M. Hodecker, Z. C. Holden, S. Houck, X. Huang, K. Hui, B. C. Huynh, M. Ivanov, Á. Jász, H. Ji, H. Jiang, B. Kaduk, S. Kähler, K. Khistyaev, J. Kim, G. Kis, P. Klunzinger, Z. Koczor-

Benda, J. H. Koh, D. Kosenkov, L. Koulias, T. Kowalczyk, C. M. Krauter, K. Kue, A. Kunitsa, T. Kus, I. Ladjánszki, A. Landau, K. V. Lawler, D. Lefrancois, S. Lehtola, R. R. Li, Y.-P. Li, J. Liang, M. Liebenthal, H.-H. Lin, Y.-S. Lin, F. Liu, K.-Y. Liu, M. Loipersberger, A. Luenser, A. Manjanath, P. Manohar, E. Mansoor, S. F. Manzer, S.-P. Mao, A. V. Marenich, T. Markovich, S. Mason, S. A. Maurer, P. F. McLaughlin, M. F. S. J. Menger, J.-M. Mewes, S. A. Mewes, P. Morgante, J. W. Mullinax, K. J. Oosterbaan, G. Paran, A. C. Paul, S. K. Paul, F. Pavošević, Z. Pei, S. Prager, E. I. Proynov, Á. Rák, E. Ramos-Cordoba, B. Rana, A. E. Rask, A. Rettig, R. M. Richard, F. Rob, E. Rossomme, T. Scheele, M. Scheurer, M. Schneider, N. Sergueev, S. M. Sharada, W. Skomorowski, D. W. Small, C. J. Stein, Y.-C. Su, E. J. Sundstrom, Z. Tao, J. Thirman, G. J. Tornai, T. Tsuchimochi, N. M. Tubman, S. P. Veccham, O. Vydrov, J. Wenzel, J. Witte, A. Yamada, K. Yao, S. Yeganeh, S. R. Yost, A. Zech, I. Y. Zhang, X. Zhang, Y. Zhang, D. Zuev, A. Aspuru-Guzik, A. T. Bell, N. A. Besley, K. B. Bravaya, B. R. Brooks, D. Casanova, J.-D. Chai, S. Coriani, C. J. Cramer, G. Cserey, A. E. DePrince, R. A. DiStasio, A. Dreuw, B. D. Dunietz, T. R. Furlani, W. A. Goddard, S. Hammes-Schiffer, T. Head-Gordon, W. J. Hehre, C.-P. Hsu, T.-C. Jagau, Y. Jung, A. Klamt, J. Kong, D. S. Lambrecht, W. Liang, N. J. Mayhall, C. W. McCurdy, J. B. Neaton, C. Ochsenfeld, J. A. Parkhill, R. Peverati, V. A. Rassolov, Y. Shao, L. V. Slipchenko, T. Stauch, R. P. Steele, J. E. Subotnik, A. J. W. Thom, A. Tkatchenko, D. G. Truhlar, T. V. Voorhis, T. A. Wesolowski, K. B. Whaley, H. L. Woodcock, P. M. Zimmerman, S. Faraji, P. M. W. Gill, M. Head-Gordon, J. M. Herbert and A. I. Krylov, *J. Chem. Phys.*, 2021, **155**, 084801.